Geochimica et Cosmochimica Acta Vol. 54, pp. 3491–3508

0016-7037/90/$3.00 + .00

Chemical compositions of siderophile element-rich opaque assemblages in an Allende inclusion

PAUL J. SYLVESTER,[1] BRIAN J. WARD,[1] LAWRENCE GROSSMAN,[1,2] and IAN D. HUTCHEON[3]

[1]Department of the Geophysical Sciences, The University of Chicago, Chicago, IL 60637, USA
[2]Enrico Fermi Institute, University of Chicago, Chicago, IL 60637, USA
[3]Lunatic Asylum of the Charles Arms Laboratory, Division of Geological and Planetary Sciences, California Institute of Technology, Pasadena, CA 91125, USA

(*Received May* 3, 1990; *accepted in revised form September* 21, 1990)

Abstract—Ten opaque assemblages, or Fremdlinge, weighing 0.17–19 μg, from an Allende Type B, Ca-, Al-rich, coarse-grained inclusion were analyzed by INAA for Ca, Na, Mn, Sc, Ta, Ti, V, Cr, Fe, Ni, Co, W, Re, Os, Ir, Mo, Ru, Pt, Rh, Au, As, Sb, and Se. Refractory siderophiles are usually enriched by factors of 10^3–10^4 relative to C1 chondrites, but not uniformly. From sample to sample, C1 chondrite-normalized Re/Os, Ir/Pt, Os/Ru, and Pt/Rh ratios vary from 0.81–1.03, 0.70–>2.25, 0.67–3.32, and 0.45–1.43, respectively. Attempts to model the abundances of refractory siderophiles by condensation from the solar nebula into a single phase, assuming ideal solution, fail to match the observed combination of subchondritic Re/Os and Ir/Pt ratios, even allowing for fractionation of the highest-temperature condensates. A different model, in which all metals whose high-temperature crystal structures are hcp condense into one alloy, bcc into another, and fcc into a third, is capable of matching virtually all refractory siderophile fractionations in these Fremdlinge. In this model, all isostructural metals are assumed to form ideal solutions with one another and metals of different structure are assumed to be insoluble in one another. After fractionation of high-temperature hcp and fcc alloys, individual proto-Fremdlinge formed by mixing of high- and low-temperature varieties of each of the three alloys, either in the nebula before and during CAI accretion, or during later partial melting of the silicate, oxide, and metal components of CAIs.

INTRODUCTION

THERMODYNAMIC CALCULATIONS suggest that many Ca-, Al-rich inclusions (CAIs) in carbonaceous chondrites formed by high temperature condensation from a cooling solar gas (GROSSMAN, 1972) and that the refractory siderophiles (W, Re, Os, Ir, Mo, Ru, Pt, Rh) within CAIs were among the earliest condensates of all (GROSSMAN, 1973; PALME and WLOTZKA, 1976). The most common occurrences of refractory siderophiles are as tiny, 0.5–5 μm single phase refractory metal nuggets (RMN) (WARK, 1986) and as larger, 10–1000 μm aggregates of metal, oxide, sulfide, and phosphate phases, called "Fremdlinge" (EL GORESY et al., 1978) or "opaque assemblages" (BLUM et al., 1989). RMN occur most commonly in Type A (fassaite-poor) inclusions, whereas Fremdlinge are more often present in Type B (fassaite-rich) inclusions. In some Type A and B inclusions, RMN and Fremdlinge occur together (EL GORESY et al., 1978; WARK, 1986).

Fremdlinge were once thought to have an origin distinct from their host CAIs, either as pre-solar grains (EL GORESY et al., 1978) or pristine nebular condensates (ARMSTRONG et al., 1985, 1987; BISCHOFF and PALME, 1987) that formed under highly oxidizing and sulfidizing conditions *before* incorporation into their inclusions. More recent evidence suggests, however, that most Fremdlinge are neither pre-solar nor pristine condensates. A study of 11 Fremdlinge in 3 Allende CAIs found no evidence for isotope anomalies in Mg, Fe, Mo, Ru, and W (HUTCHEON et al., 1987). In another study, the phase assemblages of Fremdlinge were shown to reflect low-temperature (~770 K) re-equilibration under conditions of high f_{O_2} and f_{S_2} *after* capture by their CAI hosts (BLUM et al., 1989). Fremdling precursors probably condensed from the nebular gas as submicron-sized metal alloys of refractory siderophiles which became trapped between and within the major condensing phases that accumulated to form CAIs. Later, when CAIs were partially melted under reducing conditions (BECKETT and GROSSMAN, 1986), proto-Fremdlinge formed by coalescence of immiscible liquid droplets of Fe, Ni, P, and refractory siderophiles (BLUM et al., 1989). Recently, ZINNER and EL GORESY (1990) reported evidence of O and Mg isotope anomalies in a periclase-bearing Fremdling in a CAI in Vigarano. The petrographic, chemical, and isotopic properties of this Fremdling were interpreted in terms of formation prior to incorporation into the host CAI. No Fremdlinge with similar mineralogy have been observed in Allende, and we confine our arguments to metal-, oxide-, sulfide-rich Fremdlinge characteristic of CAIs in most CV3 chondrites.

Bulk compositions of individual Fremdlinge may retain a record of the nebular condensation history of the refractory metals, if those metals were not fractionated from one another during later, low-temperature volatile alteration. It is with this reasoning that we report instrumental neutron activation analyses (INAA) of bulk Fremdlinge from an Allende CAI and, through thermodynamic modeling, attempt to constrain the nebular conditions and processes that existed during condensation of refractory siderophiles. We use the terms "opaque assemblages" and "Fremdlinge" interchangeably, and the latter only in its non-genetic, descriptive sense. Preliminary results of this study were presented by SYLVESTER et al. (1989).

ANALYTICAL METHODS

Sample Preparation for INAA

Nine Fremdlinge were separated from the Allende Type B CAI, Egg 6 (MEEKER et al., 1983), at Caltech. A portion of the inclusion,

~3 g, was gently crushed into coarse fragments using stainless steel tools. The mm-diameter Fremdling, Zelda (ARMSTRONG et al., 1987), was recovered at this stage. Crushing continued until the majority of the material passed through a 300 μm mesh. The sieved material was passed through a magnetic separator and the Fremdlinge were hand-picked from the most magnetic fraction using stainless steel tweezers under a binocular microscope. The Fremdlinge were attached to a scanning electron microscope (SEM) sample mount using double-sided adhesive tape, and carbon-coated for preliminary characterization using the SEM. Following this study, the Fremdlinge were mailed to the University of Chicago still attached to the SEM mount. The Fremdlinge were picked off the mount using stainless steel forceps which had been dipped in acetone to dissolve adhesive attached to the Fremdlinge. Each sample was then placed in an HNO_3-washed, aluminum-foil boat and weighed ten times with a Perkin-Elmer AD-2Z electronic microbalance. Weights are given in Table 1. One sample, F6, was not weighed because all of the adhesive tape could not be removed from it. A weight of 0.5 μg was assumed for F6, based on its volume.

We attempted to retrieve samples that are representative of bulk Fremdlinge, but we cannot be sure that this was the case. Fremdlinge are heterogeneous assemblages that are difficult to remove completely from their silicate hosts (ARMSTRONG et al., 1987). Some Fremdlinge fragmented during crushing and sieving. Also, some of the specimens were broken into several fragments on the adhesive tape, and it was possible to retrieve many, but not all, of the chips. We indicate which assemblages are complete objects and which are fragments in sample descriptions presented later.

After weighing, the Fremdlinge were loaded into supersilica tubes that had been cleaned in aqua regia. The tubes were then sealed, washed in aqua regia, rinsed with distilled water, and dried. The tube containing F5 was dropped before it was sealed and some of the sample was lost. The weight of F5 was assumed to be 0.5 μg.

A number of solid standards were weighed into supersilica tubes. These included powders of BCR-1, the Standard Pot SP (PERLMAN and ASARO, 1969, 1971) and Johnson-Matthey Specpure TiO_2, and a small chip of the well-analyzed group IIAB hexahedrite, Filomena (WASSON et al., 1989), used as a secondary standard for refractory siderophiles. Aliquots of several liquid standards were micro-pipetted into supersilica tubes, weighed, and evaporated to dryness before sealing. These included the SPEX Industries Plasma Standards for Mo, Rh, and W as well as one group chemical standard, NZ, containing Ni, Zn, Se, Pt, and Pd, prepared as in DAVIS et al. (1982), and another, AR, containing Au, Ir, Re, Os, and Ru, prepared as in MAO et al. (1990). Two empty tubes were included as blanks. Supersilica tubes for standards, flux monitors, and blanks were sealed and cleaned by the same procedure used for the tubes containing Fremdlinge.

Irradiation and Counting

Two irradiations were performed. In a rabbit irradiation, samples and standards (BCR-1, SP, TiO_2, Filomena, and Rh) were individually subjected to a neutron flux of 5×10^{13} n/cm^2/sec for 5 min in the first row of the graphite reflector of the University of Missouri Research Reactor (MURR) using a pneumatic transfer system. After irradiation, each tube was taped to an aluminum card and counted twice on an 11.6% efficiency Ge(Li) detector for ^{52}V ($t_{1/2}$ = 3.76 min), ^{104m}Rh (4.36 min), and ^{51}Ti (5.76 min). As Si interferes with Al, and Al with Mg, neither Al nor Mg were determined because the samples were irradiated in supersilica tubes. We did not use polyethylene pouches, as we were primarily interested in refractory siderophiles, most of which are determined in the long irradiation, and we did not wish to risk sample loss during transfer from pouches to tubes. In the first count, 2.2–9.0 min after irradiation, spectra were acquired for 3.0–5.7 min each. In the second count set, 4.3–29 min after irradiation, the samples were moved closer to the detector, and spectra were acquired for 3.0–7.0 min each. Two slightly longer-lived isotopes, ^{56}Mn ($t_{1/2}$ = 154.74 min) and ^{24}Na (898.2 min), were counted 170–570 min after irradiation on Ge(Li) detectors with efficiencies of 28.1 and 35.5%. Spectra were acquired for 10–20 min.

Eight Co-doped aluminum wires irradiated during the rabbit experiment indicated that the neutron flux had increased 2.2% by the time the last tube had been irradiated. Corrections were made to each sample and standard accordingly. Room background was measured on each of the three detectors at MURR, but none of the short-lived radioisotopes of interest were observed. Sodium and manganese were present in the blank supersilica tubes. Two Fremdlinge (F5, F10) had Na peaks after blank corrections amounting to 18–19% of the total Na present. For the other samples, Na blanks exceed 100% of

Table 1. Element Concentrations in Fremdlinge

	mass(μg)	Fe(%)	Ni(%)	Ti(%)	V(%)	Cr(%)	Mn(%)	Na(%)	Ca(%)	Sc	Co	Ta	W
F1	20.0 ± 0.3	11.51 ± 0.04	2.01 ± 0.02	1.22 ± 0.13	1.37 ± 0.02	0.553 ± 0.003	0.00525 ± 0.00020	< 0.041	13.7 ± 0.5	195.9 ± 0.1	1398 ± 4	< 0.14	58.0 ± 0.5
F2	1.3 ± 0.3	46.9 ± 0.2	15.57 ± 0.09	< 2.7	1.27 ± 0.03	1.729 ± 0.009	0.121 ± 0.004	< 0.056	< 3.6	27.8 ± 0.1	6990 ± 20	< 0.82	491 ± 3
F4	2.5 ± 0.5	41.7 ± 0.2	26.7 ± 0.1	< 1.5	1.12 ± 0.02	0.965 ± 0.031	0.0502 ± 0.0018	< 0.11	3.4 ± 1.3	4.62 ± 0.07	7070 ± 20	< 0.82	5.8 ± 1.1
F5	0.5[1]	73.7 ± 0.3	4.58 ± 0.05	< 11	0.154 ± 0.045	34.82 ± 0.09	3.41 ± 0.05	12.2 ± 0.5	1.49 ± 0.57	0.96 ± 0.38	701 ± 18	< 0.74	40.0 ± 2.5
F6	0.5[1]	201.9 ±0.6	20.9 ± 0.2	< 7.9	0.371 ± 0.039	17.27 ± 0.04	2.77 ± 0.03	< 0.36	11.4 ± 2.1	17.5 ± 0.4	8310 ± 30	< 1.4	131 ± 3
F9	10.5 ± 0.4	35.5 ± 0.2	30.9 ± 0.2	< 0.28	1.96 ± 0.03	2.07 ± 0.01	0.00208 ±0.00024	< 0.051	< 3.2	7.17 ± 0.09	7630 ± 30	< 1.0	14.2 ± 1.0
F10	1.6 ± 0.3	37.3 ± 0.1	8.70 ± 0.04	< 2.8	1.94 ± 0.04	1.021 ± 0.006	0.0069 ± 0.0014	2.96 ± 0.13	< 1.3	8.12 ± 0.10	3780 ±10	< 0.47	< 4.3
F11	2.1 ± 0.3	58.1 ± 0.1	3.13 ± 0.03	< 1.7	0.359 ± 0.012	0.594 ± 0.005	0.0148 ± 0.0013	< 0.10	2.29 ± 0.49	4.86 ± 0.06	1484 ± 6	0.425 ± 0.087	10.7 ± 0.8
F12	0.4 ± 0.2	12.2 ± 0.2	20.7 ± 0.2	< 2.2	< 0.11	0.951 ± 0.030	0.0172 ± 0.0053	< 0.33	< 5.1	< 0.95	9340 ± 40	41.6 ± 1.1	< 11
Zorba	18.2 ± 0.3	39.1 ± 1.7	29.1 ± 0.2	< 0.10	0.874 ± 0.017	0.60 ± 0.08	0.0030 ± 0.0014	0.044 ± 0.013	1.39 ± 0.20	5.5 ± 1.4	7950 ± 290	---	< 210
Filomena (this study)	1409.3 ± 0.2	95.7 ± 0.3	5.64 ± 0.02	< 0.0051	0.00006 ± 0.00002	0.0068 ± 0.0001	0.00077 ± 0.00001	0.0051 ± 0.0002	< 0.18	< 0.0064	4600 ± 20	< 0.037	---
Filomena (previous [2])		---	5.65 ± 0.06	---	---	0.0068 ± 0.0009	---	---	---	---	4540 ± 50	---	2.562 ± 0.013
Isotope		^{59}Fe	^{58}Co	^{51}Ti	^{52}V	^{51}Cr	^{56}Mn	^{24}Na	^{47}Ca	^{46}Sc	^{60}Co	^{182}Ta	^{187}W
Half-Life		44.5d	70.9d	5.76m	3.76m	27.7d	2.58h	15.0h	4.54d	83.8d	5.27y	114d	23.9h
Energy (keV)		1099	810	320	1434	320	846	1368	1297	889	1173	1221	686
Standard		SP	NZ	Chem	BCR	SP	BCR	SP	BCR	SP	SP	SP	Filomena

Notes: All units in ppm unless otherwise indicated. Quoted uncertainties for each concentration are based on 1 σ counting statistics errors.
[1] Assumed mass. [2] Wasson *et al.* (1989) unless otherwise noted. [3] Absolute concentrations of Ir, Au, Re, Os and Ru in chemical standard AR uniformly increased by 13.3 % to bring the absolute concentrations of Re, Au and Ir in Filomena more in line with the values of Wasson *et al.* (1989). [4] Pernicka and Wasson (1987). [5] Wasson and Wang (1986). [6] Herr *et al.* (1961). [7] Smales *et al.* (1967). [8] Hara and Sandell (1960). [9] Nichiporuk and Brown (1965). [10] Willis (1981). See text for irradiations used.

the total Na, and Na data are, thus, reported as upper limits. Mn blank corrections were 5% or less for all Fremdlinge, except F9 (19%), F10 (30%), and F12 (48%).

A second irradiation was performed to determine longer-lived isotopes, listed in Table 1. After being washed in warm aqua regia and rinsed in double-distilled water, the tubes containing the samples and Filomena which had been used in the rabbit irradiation were sealed in groups of 5 or 6 in larger, 4 cm long supersilica tubes, as were additional small tubes containing fresh standards (BCR-1, SP, Mo, W, NZ, and AR). A tube containing a fresh piece of Co-doped aluminum wire was included in each large tube to monitor the spatial variation of the neutron flux. The large tubes were wrapped in a bundle and irradiated together in the first row of the graphite reflector of MURR for 206.3 h at a flux of 8×10^{13} n/cm^2/sec. The tubes were individually washed in warm aqua regia and mounted on aluminum cards. Two high purity Ge detectors with efficiencies of 35.7% and 37.9% were used to count the samples at the University of Chicago. Each Fremdling was counted three times: for 1.75–7.0 h, 15.6–37.4 h after irradiation; for 13.2–28.4 h, 4.7–8.4 days after irradiation; and for 5.8–7.1 days, 40.2–67.2 days after irradiation. Standards and blanks were also counted three times, after each of the Fremdling count sets. Count times for standards and blanks were comparable to count times for samples.

Data Reduction for Long Irradiation

Corrections for the spatial variation of neutron flux of ≤3.9% were made to each sample and standard. Because of the large neutron capture cross section of ^{198}Au, significant burn-out of ^{198}Au, used for determining Au, and production of ^{199}Au, used for determining Pt, occur in high-fluence irradiations via ^{197}Au(n, γ)^{198}Au(n, γ)^{199}Au. Resulting deviations from linear dependence of specific activity on fluence were taken into account in flux corrections for these nuclides produced from ^{197}Au. The following elements were undetectable in the blanks: Re, Os, Ir, Ru, Pt, Mo, Au, Ca, Ta, and Se. Blank corrections were necessary for ^{51}Cr (≤6.6% of the total counts in each sample), ^{59}Fe (≤7.0%), ^{58}Co (≤5.1% except 15% in sample F5), ^{46}Sc (≤8.2% except 62% in F5), ^{60}Co (≤1.0% except 9.6% in F5), ^{187}W (≤18% except 39% in F11, 43% in F5, and 50% in F4), ^{76}As (≤16% except 29% in F1, 50% in F2, and 86% in F6), and ^{124}Sb (36% in F5, 63% in F6, and 33% in F11). Blank corrections tend to be largest for sample F5 because of its small mass and low siderophile element contents.

Arsenic was determined from ^{76}As at 559 keV. A correction was made for ^{193}Os, which also decays with this energy. The ratio of ^{193}Os counts at 559 keV to ^{193}Os counts at 460 keV in an As-free, Os standard was multiplied by the ^{193}Os counts at 460 keV in the samples. This number was subtracted from the total counts at 559 keV in the samples; the correction amounted to 0–68% of the total counts. Selenium was measured from ^{75}Se at 264 keV, but two Fremdlinge (F11 and F12) were found to contain ^{182}Ta, which interferes with this determination. The ratio of ^{182}Ta counts at 264 keV to those at 1221 keV in a Se-free, Ta standard was used to make corrections of 0.1 and 3.6% in the two Fremdlinge, respectively. Platinum concentrations were determined after subtraction of the contribution of Au to the total ^{199}Au counts. In Fremdlinge, this contribution was 21–92%.

Uncertainties due to counting statistics (1σ) for all peaks used in the determination of an element were propagated into the error for that element in every sample.

Analytical Technique for Zorba

In our study of opaque assemblages from Egg 6, we also include Zorba, a large (200 μm diameter) Fremdling from the same inclusion. Zorba was analyzed previously in this laboratory (GROSSMAN et al., 1986) using standards and experimental procedures described by EKAMBARAM et al. (1984). In the rabbit irradiation used by GROSSMAN et al. (1986), Zorba was irradiated for 6 min at a flux of 8.8×10^{13} n/cm^2/sec in the first row of the graphite reflector at MURR. It was counted twice, 2.5 min after irradiation for 500 sec and 6 h after irradiation for 1000 sec. In the long irradiation of that study, Zorba was placed in the flux trap at MURR and irradiated for 290.93 h at 3.8×10^{14} n/cm^2/sec. Three counts were made, 5.1 days after irradiation for 3.1 h, 26 days after irradiation for 2.2 h, and 57 days after irradiation for 19.5 h.

Sample Characterization

After INAA, 7 samples were retrieved from their supersilica vials, mounted in epoxy, polished, and examined with a JEOL JSM-35CF SEM equipped with a Tracor TN-5500 energy dispersive X-ray spectrometer (EDS). Quantitative X-ray chemical analyses were performed at 15 keV and 60 pa, and the data were corrected using the α-factor procedure of BENCE and ALBEE (1968) and ZAF procedures of LOVE and SCOTT (1978) and PACKWOOD and BROWN (1981), as modified

Table 1 (cont.)

	Re	Os	Ir	Mo	Ru	Pt	Rh	Au	As	Sb	Se
F1	47.6 ± 0.9	633 ± 1	495 ± 1	5570 ±170	812 ± 3	1050 ± 30	133 ± 13	29.26 ±0.07	2.26 ± 0.30	< 0.29	20.6 ± 1.2
F2	234 ± 3	3739 ± 8	3530 ± 10	8700 ± 470	6170 ± 20	10300 ± 100	1230 ± 120	23.8 ± 0.1	14.3 ± 1.1	< 1.2	195 ± 9
F4	395 ± 6	6270 ± 10	5450 ± 20	13600 ± 500	5330 ± 20	8770 ± 230	1260 ± 70	257.4 ± 0.6	57 ± 12	< 1.3	113 ± 10
F5	4.24 ± 0.51	67.1 ± 1.9	20.36 ± 0.09	174 ± 57	144 ± 3	< 20	< 1500	2.23 ± 0.02	< 7.7	7.2 ± 1.4	< 9.2
F6	138 ± 3	2205 ± 8	2473 ± 7	3780 ± 450	2690 ± 20	5830 ± 90	960 ± 360	58.4 ± 0.2	< 7.0	< 2.3	149 ± 6
F9	496 ± 22	7710 ± 20	7000 ± 50	18200 ± 1800	5000 ± 20	9900 ± 700	1510 ± 40	318 ± 2	15.0 ± 1.2	< 1.1	35 ± 13
F10	146 ± 3	1886 ± 3	997 ± 3	< 200	2190 ± 7	1030 ± 20	310 ± 90	20.52 ± 0.06	< 3.9	< 0.72	41.2 ± 4.0
F11	139 ± 2	2282 ± 4	2329 ± 6	710 ± 110	2232 ± 9	5250 ± 110	497 ± 64	155.7 ± 0.3	44.8 ± 1.3	1.02 ± 0.27	67.1 ± 5.8
F12	451 ± 5	7260 ± 20	6860 ± 20	1500 ± 360	8110 ± 40	8340 ± 360	1150 ± 370	542 ± 1	391 ± 9	< 2.9	< 76
Zorba	825 ± 25	13400 ± 300	15400 ± 20	44800 ± 4900	5900 ± 100	---	---	590 ± 4	< 79	< 4.8	860 ± 240
Filomena (this study)	0.230 ± 0.026	1.06 ± 0.07	3.44 ± 0.03	< 17	17.6 ± 0.4	20.0 ± 1.5	< 1.4	0.609 ± 0.004	4.96 ± 0.33	< 0.040	< 0.28
Filomena (previous[2])	0.234 ± 0.014	1.14-1.3 [4-6]	3.37 ± 0.05	6.9-7.2 [7]	14.2-21.5 [4, 8, 9]	20.7 ± 0.7	2.5 [9]	0.612 ± 0.008	4.73 ± 0.09	0.048-0.11 [7, 10]	---
Isotope	^{188}Re	^{191}Os	^{192}Ir	^{99}Mo	^{103}Ru	^{199}Au	^{104m}Rh	^{198}Au	^{76}As	^{124}Sb	^{75}Se
Half-Life	17.0h	15.4d	74.2d	65.9h	39.2d	3.14d	4.36m	2.69d	26.3h	60.2d	120d
Energy (keV)	155	129	468	739	497	158	51.4	412	559	1691	264
Standard	AR[3]	AR	AR	Chem	AR	NZ	Chem	AR	SP	SP	NZ

by ARMSTRONG (1982, 1984). For Ru and Mo, the L_α X-ray lines were used for quantitative analysis, whereas for Re, Os, Ir, and Pt, the M_α lines were used. A more detailed discussion of the analytical procedures is given by ARMSTRONG et al. (1985).

RESULTS

SEM Petrography of Analyzed Fremdlinge

F1

In this and all other Fremdling descriptions, modal percentages are expressed in wt%. Originally spheroidal, ~180 μm in diameter, only about one-half of this Fremdling was recovered from the host inclusion; the polished surface has a semicircular cross-section, ~180 × 85 μm. The most striking feature is a large region of molybdenite (MoS_2), ~45 × 60 μm, located near the center and occupying ~23% of the sample. The remainder of the assemblage is predominantly pentlandite (33%), pyrrhotite (25%), Fe-, Mg-silicate (6%), apatite (4%), V-rich magnetite (6%), and NiFe metal (4%). Submicron-sized OsRu nuggets are concentrated in pentlandite and MoS_2. Larger, 1–2 μm, blebs of NiFe contain up to 30% Pt and occasionally surround OsRu nuggets. The assemblage is separated from its melilite host by a rim of V-rich, Ti-poor fassaite and rare, V-rich spinel. Also found in the host melilite, ~250 μm from this large Fremdling, are two smaller opaque assemblages. The larger one, ~30 μm across, is predominantly pyrrhotite with minor magnetite and a 3 × 10 μm crystal of MoS_2. The other, ~20 μm away, contains no sulfide and is composed of NiFe and magnetite.

F2

This Fremdling, 50 × 75 μm, is composed predominantly of a wormy intergrowth of pentlandite (72%) and Fe-rich silicate ($Ca(Mg_{0.65}Fe_{0.35})SiO_4$; 23%). Pentlandite is concentrated around the periphery, and the Fe-silicate is most abundant in the interior. Cr-, V-rich magnetite, MoS_2, pyrrhotite, olivine (~Fo_{64}), and apatite are minor phases (~2%). Metal nuggets scattered throughout pentlandite contain nearly equal atom fractions of Ru and Os and ~25% as much Ir. No NiFe is present.

F4

This Fremdling, 130 × 130 μm, is composed predominantly of pentlandite (48%) and NiFe (46%) which occur in distinct, relatively coarse-grained regions and are not extensively intergrown. MoS_2 (2%) occurs as one relatively large (10 × 20 μm) crystal and numerous small blades. Small crystals of V-rich magnetite (3%) are included in pentlandite. F4 is one of only two Fremdlinge (F9 being the other) to have both apatite and whitlockite. The phosphates and pyrrhotite are minor phases. The majority of submicron-sized RMN are OsRu. Four larger RMN exhibit extreme segregation of Pt-group metals. Three consist of Pt with no Ir, the other of Ir with no Pt.

F9

Originally spheroidal, ~200 μm in diameter, this sample was very friable and broke into several pieces. All fragments were irradiated and counted together. The two largest pieces, 9A and 9B, were mounted separately and yielded polished sections, each ~150 × 180 μm, which are strikingly different in appearance and composition from one another. Assemblage 9A is composed primarily of pentlandite (60%), NiFe metal (32%), Ca-phosphate (4%), and pyrrhotite (2%). The central region contains abundant voids that occupy ~25% of the exposed area and give the assemblage a lacy texture. Minor phases are V-, Cr-rich magnetite as thin rims (1–2 μm) around pentlandite and NiFe metal; molybdenite as bladed crystals, 1–2 μm across and 5–10 μm in length; and micron-sized OsRu nuggets. At pentlandite-NiFe boundaries, irregular blebs of NiFe contain up to 30% Pt.

Assemblage 9B is composed primarily of pyrrhotite (43%), pentlandite (21%), NiFe metal (28%), and an Fe-, Mg-silicate (5%). Pyrrhotite is concentrated in a 20–30 μm wide mantle surrounding the assemblage but also occurs as isolated 5–10 μm crystals in the interior. Pentlandite is found exclusively in the interior, commonly associated with NiFe metal. NiFe metal is also concentrated in the interior, but a few crystals are scattered throughout the pyrrhotite mantle. The Fe-, Mg-silicate fills interstitial spaces between sulfide crystals, giving fragment 9B a much less porous appearance than 9A. Larger (5–10 μm) crystals of this phase are concentrated around the margin of the Fremdling. A 15 μm diameter olivine crystal (Fo_{75}) is embedded in the pyrrhotite mantle. Minor constituents are molybdenite, V-, Cr-rich magnetite, and submicron-sized OsRu nuggets. Curiously, MoS_2 is a prominent constituent of neither 9A nor 9B, despite the fact that crystals up to 20 × 70 μm were seen on the original surface of the Fremdling during its recovery from Egg 6.

F10

This greenish Fremdling is rectangular in polished section, ~80 × 190 μm, suggesting that it is a fragment of a once larger object. Pentlandite (47%) occurs as coarse grains, up to 30 μm across, intergrown with smaller (2–10 μm) crystals of V-rich magnetite (15%), NiFe metal (17%), pyrrhotite (17%), and Ca-phosphate (3%). This Fremdling is notable for the absence of MoS_2 and RMN.

F11

This Fremdling, 80 × 100 μm, consists of pyrrhotite with minor apatite, Ti-, V-, Cr-rich magnetite, pentlandite, and Fe-rich silicate ($Ca(Mg_{0.6}Fe_{0.4})SiO_4$). Numerous submicron-sized OsRu nuggets and a few 1–2 μm nuggets of OsIr are scattered throughout the pyrrhotite. Apatite, magnetite, and pentlandite occur as isolated patches, 2–8 μm in size, enclosed in pyrrhotite. The Fe-silicate occurs as a wormy intergrowth with pyrrhotite at one end of the assemblage.

Zorba

This Fremdling is roughly spherical, ~200 μm in diameter, and is composed primarily of pentlandite (44%), pyrrhotite (22%), NiFe metal (24%), molybdenite (4%), apatite (2%), Fe-, Mg-silicate (1%), V-, Cr-rich magnetite (2%), and RMN of OsRu (1%). These phases are distributed asymmetrically within Zorba. Pentlandite and pyrrhotite are finely intergrown, with crystal sizes ≤ 10 μm. Pentlandite around the margin of the assemblage contains ~12% Ni, while that

in the interior contains ~27% Ni. NiFe metal occurs as isolated crystals, 10–30 μm in size, in pentlandite. Metal grains have highly embayed edges and are frequently associated with blebs of Pt-rich metal. One large (15 × 60 μm) crystal of MoS_2 projects inward normal to the edge of Zorba. Apatite occurs primarily as narrow laths, ~2 μm wide and up to 20 μm long. Most of the laths exhibit a preferred orientation approximately normal to the MoS_2 crystal. Fe-, Mg-silicate is concentrated at one end of Zorba, as a few, 10 micron-sized, rounded crystals. V-, Cr-rich magnetite occurs as 1–3 micron-sized crystals distributed throughout pentlandite. Submicron-sized RMN are concentrated in pentlandite at one end of Zorba, and a few, 1–2 micron-sized RMN occur at the opposite end, associated with NiFe metal.

INAA Data

The results of the INAA experiment are presented in Table 1, along with the isotope, half-life, γ-ray energy, and standard used to determine each element in the rabbit and long irradiations. The 1σ uncertainties are based on counting statistics alone. An additional uncertainty of ±1–5% is possible in the absolute concentrations due to counting geometry differences between samples and standards, but this effect will be the same for all elements in the same sample. Also shown in Table 1 are the results for Filomena, compared to previous analyses. There is generally good agreement between the two data sets. For W, however, our chemical standard gave a concentration for Filomena that is 14% greater than the "best" value of WASSON et al. (1989) and 8–11% greater than the data of ATKINS and SMALES (1960), so the WASSON et al. (1989) determination for Filomena was used as our standard. Our chemical standard AR gave concentrations for Re, Au, and Ir in Filomena that are 13.3, 13.6, and 13.0% lower, respectively, than those of WASSON et al. (1989). The uniform depletion of these elements suggests that the weight of the AR standard was ~13.3% higher than the value we measured. The weight was, therefore, increased accordingly for analysis of all Fremdlinge except Zorba. Os and Ru, which are also in the AR standard, but which were not analyzed by WASSON et al. (1989), give standard-renormalized values for Filomena that are comparable to those reported by other laboratories (Table 1). Our values for Os, 1.06 ± 0.07, and Ru, 17.6 ± 0.4, are particularly close to the most recent data of PERNICKA and WASSON (1987), 1.14 ppm Os and 19.3 ppm Ru.

The element concentrations given in Table 1 for Zorba are those reported in GROSSMAN et al. (1986), except for Re, Ir, Ru, and Au, for which the chemical standards used in that work were inferior. One of the standards contained Au, Ir, and Re and the other contained Os and Ru. When subsequently measured against a different aliquot of the AR standard from that discussed above, these older standards were found to have 63% of the Re, 88% of the Os, 77% of the Ir, 67% of the Ru, and 65% of the Au relative to the concentrations assumed in the Zorba irradiation. Observed differences between the previously accepted and AR-standardized Au/Ir and Os/Ru ratios in the older standards cannot be due to weighing errors. It was, therefore, assumed that, perhaps due to age, the integrity of the older standards had deteriorated by different amounts for each element and that Os, whose previously accepted and subsequently measured abundances are most similar, is correct in the older standards. The concentrations of Re, Ir, Ru, and Au in Zorba were renormalized relative to Os, based on their depletion factors measured by the AR standard.

Recalculation of Sample Weights

The mineral modes of the Fremdlinge studied here were calculated from their bulk compositions determined by INAA for several reasons. First, some major elements in our samples, Al, Mg, Si, P, S, and O, were not determined by INAA. Calculation of mineral modes from elements which are determined by INAA can be used to estimate concentrations of those which are not. Second, due to their small sizes, the weight of one sample, F12, was poorly determined, and the weights of two others, F5 and F6, were only estimated. From the masses of elements determined by INAA, mineral modes can be used to calculate the masses of other elements present, providing for these samples a better estimate of the total sample weight upon which element concentrations can be based. A sample weight was similarly calculated for each of the other seven Fremdlinge and compared to the measured weight. Third, since petrographic observations were made on only seven of our samples, calculated modes provide important mineralogical information on the others. Calculated modes can be checked for accuracy by comparison with actual mineralogical compositions for those samples which were studied by SEM, although a particular section through a heterogeneous Fremdling may not be representative of its bulk. Fourth, some of our Fremdlinge contain attached silicates from their CAI host. Mineral modes allow recalculation of element concentrations in the Fremdlinge themselves on an attached silicate-free basis. One assumption made in doing this is that V-rich spinel is not an attached host phase. This phase rims Fremdlinge and probably formed by reaction of V from Fremdlinge with spinel from the CAI host (ARMSTRONG et al., 1987), but we have no way of estimating its abundance or the masses of Mg, Al, and O contributed by it. Another assumption is that fassaite and melilite, which are found elsewhere in Egg 6 (MEEKER et al., 1983), and nepheline, which was found on the exterior surface of some Fremdlinge during the preliminary SEM study, are attached silicates which should be subtracted when calculated to be present. In contrast, Fe-silicate, which is not found elsewhere in the inclusion, is assumed to be an indigenous phase in Fremdlinge and is not subtracted.

For each sample, the calculation was done by solving a family of mass-balance equations that uniquely defines the modal mineralogy. In each equation, the concentration of an element in a sample, as determined by INAA (Table 1), equals the sum of the products of the fraction of each phase containing that element in the sample and the concentration of that element in that phase. Equations were written only for elements that are major constituents of phases thought to be present (e.g., Fe, Cr, and V in magnetite; Fe and Ni in metal and pentlandite; Na in nepheline). The calculated mode was then checked for consistency with the abundances of other elements.

Representative mineral compositions used in this calculation are given in Tables 2 and 3. They were determined by SEM/EDS analyses of five of the seven opaque assemblages studied petrographically after INAA. Since the compositions of some phases are not constant from one assemblage to another, the calculation used compositions measured in each Fremdling except in the cases of F5, F6, F10, F11, and F12. Quantitative analyses were not obtained for the latter, so average phase compositions from the other Fremdlinge were used. A stoichiometric composition was used for nepheline in F5 and F10. The high Na contents determined by INAA for these two inclusions allow large amounts of nepheline, but SEM study suggests that no more than 10% nepheline is present. We, thus, assumed that 10% nepheline was present and that the excess Na was the result of laboratory contamination. In order to obtain the proportions of Fe-silicate, apatite, and whitlockite, we had to ignore olivine in F2 and F9 and apatite in F2, F4, and F9 in our calculations. For F1, F10, F11, and Zorba, we had to assume that the amounts of Fe-silicate and apatite were those observed by SEM/EDS. No successful solutions for the modes of F5 and F6 could be found using the high Cr concentrations, 34.8 and 17.3%, respectively, determined by INAA. For each of these

Table 2. Compositions of Metal and Sulfide Minerals in Egg 6 Fremdlinge (wt. %)

	NiFe Metal		Pyrrhotite		Pentlandite		Molybdenite		Ptlr RMN[1]		OsRu RMN[1]	
	Mean	Range	Mean	Range	Mean	Range	Mean	Range	Mean	Range	Mean	Range
S	---	---	37.3	36.7-37.8	33.2	31.0-36.1	39.6	39.1-39.8	---	---	---	---
Cr	0.2	0.1-0.4	0.2	0-0.4	0.2	0-0.6	0.2	0-0.4	0.2	0-0.4	0.1	0-1.9
Fe	29.8	29.1-32.6	60.7	58.6-62.0	42.9	36.4-49.5	1.0	0.5-1.3	32.2	31.8-33.0	13.3	7.1-23.1
Co	1.8	1.3-2.4	0.2	0-1.8	1.1	0.5-1.7	---	---	1.0	0.7-1.3	0.2	0-0.4
Ni	62.5	60.1-65.2	0.1	0.1-1.4	21.6	12.7-29.5	---	---	29.3	28.7-31.0	4.2	1.8-9.1
Mo	---	---	---	---	---	---	58.2	57.4-59.3	---	---	---	---
Ru	0.3	0-1.5	0.6	0.3-1.2	1.0	0.1-1.6	---	---	---	---	28.3	11.7-44.5
Re	---	---	---	---	---	---	---	---	---	---	2.3	1.0-7.5
Os	0.2	0-0.7	---	---	---	---	---	---	---	---	47.5	36.1-56.7
Ir	1.6	0.9-3.6	---	---	---	---	0.6	0-0.8	5.9	5.7-6.3	2.8	1.0-8.5
Pt	2.8	1.1-6.2	---	---	---	---	---	---	31.5	30.3-32.0	---	---
Total	99.2		99.1		100.0		99.6		100.1		98.7	

[1]Since RMN are typically submicron-sized, analyses originally included contributions from surrounding phases. Deconvolution for RMN in pentlandite or pyrrhotite assumed all S present in sulfide, while for RMN in NiFe, deconvolution minimized Ni in RMN consistent with NiFe composition.

samples, we disregarded our Cr datum and calculated the mass of Cr from the mode. The high values found in F5 and F6 may be due to laboratory contamination, although a specific source has not been identified. The derived mineral modes for all Fremdlinge are shown in Table 4.

As expected, the sums of the weights of phases calculated to be present in samples with poorly measured or estimated weights, F5, F6, and F12, differ greatly from the measured or estimated values, totalling 206, 380, and 42%, respectively, of the latter. We adopted the calculated weights. For each of the other samples, except F10 and Zorba, the sum of the weights of phases in the calculated mode summed to an amount that was within error of the measured weight. We also adopted the calculated weights of these samples.

Calculated Mineralogy

Calculated mineralogical compositions of the Fremdlinge from Egg 6 are extremely variable (Table 4). NiFe metal ranges from 0% in four Fremdlinge to 74 wt% in F12. RMN range from 0% in F10 to 3% in F12. Calcium-phosphate varies from 0% in F2 to 5% in F6 and F12. Iron-silicate varies from 1% in F10 to 14% in F2. Attached silicate was calculated in three samples: F1, F5, and F10. All Fremdlinge, except F12, are sulfide-rich, like Zelda (ARMSTRONG et al., 1987). F9 has the most magnetite (23%), much less than Willy (50%), an oxide-rich Fremdling described by ARMSTRONG et al. (1985) from Allende CAI 5241.

Calculated mineral modes compare favorably to those determined from petrography in samples F2, F11, and Zorba. In F2, pentlandite is both calculated (78%) and estimated from SEM backscattered electron images (72%) to be the most abundant phase. Iron-silicate is the next most abundant phase, although the SEM/EDS estimate (23%) exceeds the calculated estimate (14%). Even the calculated amount of Fe-silicate may be too high, as it was derived from an INAA upper limit of <3.6% for Ca. We suspect that Fe-silicate is over-represented in the polished section compared to the bulk sample. In F11, pyrrhotite is the most abundant phase in the section and in the calculated mode (77%). In Zorba, there is 22% pyrrhotite, as determined by both calculation and SEM/EDS. Calculated and SEM/EDS estimates for NiFe metal, molybdenite, and magnetite are also close: 35 vs. 24%, 7 vs. 4%, and 7 vs. 2%, respectively. Only the calculated (22%) and SEM/EDS (44%) estimates of pentlandite are greatly different.

For sample F1, both the calculated and SEM/EDS estimates of the mode find pentlandite to be the most abundant phase, 35 vs. 33%, respectively. Also, NiFe metal is absent from the calculated mode and comprises only 4% of the section. The SEM/EDS estimate of the amount of molybdenite is much larger (22%) than calculated (4%). The section of F1 intersects a particularly large molybdenite crystal parallel to the base of a plate. Because these plates are usually much larger parallel to the base than perpendicular to it, the large areal abundance of molybdenite in this section is probably an overestimate of its volume abundance. The calculated amount of fassaite (26%) is derived from the total Ti content of F1 (1.2%), after subtracting the amount contributed by magnetite, assumed to be the only other Ti-bearing phase present. Given this amount of fassaite, the above assumptions and the total Ca content of F1, 40% melilite is calculated to be present. The calculated amount of magnetite (22%) is greater than the observed amount (6%), possibly due to the fact that some V is present in spinel, which is not included in the calculation (see below).

In F4, we calculate 61% pentlandite and 18% NiFe metal, while 48% pentlandite and 46% NiFe are estimated by SEM/EDS. In addition, we calculate 4.5% whitlockite and 7% Fe-

Table 3. Compositions of Silicate and Oxide Minerals in Egg 6 Fremdlinge (wt. %)

	Magnetite		Whitlockite		Apatite		Fe-,Mg-Silicate		Fassaite		Olivine	
	Mean	Range	Mean	Range	Mean	Range	Mean	Range	Mean	Range	Mean	Range
Na_2O	---	---	2.5	2.0-2.8	---	---	0.2	0-0.6	---	---	---	---
MgO	1.8	0.5-3.0	2.5	2.0-3.0	---	---	15.0	13.2-16.8	10.7	8.2-13.3	45.7	43.1-48.2
Al_2O_3	5.0	2.4-6.5	0.2	0-0.3	---	---	---	0-0.2	13.0	6.5-17.0	---	---
SiO_2	---	---	---	---	---	---	34.7	34.1-35.1	42.4	36.8-47.0	39.5	38.0-40.7
P_2O_5	---	---	44.6	42.8-46.7	42.7	40.0-43.5	---	---	---	---	---	---
Cl	---	---	---	---	0.5	0.3-0.7	---	---	---	---	---	---
CaO	---	---	45.1	42.1-48.0	53.8	51.8-54.6	32.8	32.2-33.4	25.2	24.0-25.9	0.7	0.2-1.3
TiO_2	0.7	0-1.2	---	---	---	---	---	---	4.8	0.8-10.9	---	---
V_2O_3	21.7	11.2-34.2	---	---	---	---	---	---	2.7	0.7-6.8	---	---
Cr_2O_3	8.4	4.5-13.1	0.1	0-0.7	---	---	0.4	0.2-0.8	0.2	0-0.4	0.2	0-0.4
FeO	32.4	28.5-36.0	5.5	3.7-6.5	2.1	1.5-4.2	17.3	15.6-19.1	0.5	0.2-0.7	14.3	11.2-17.3
Fe_2O_3	28.3	26.1-30.5	---	---	---	---	---	---	---	---	---	---
NiO	2.0	1.1-3.4	---	---	---	---	---	---	---	---	---	---
Total	100.3		100.5		99.1		100.4		99.5		100.4	

Table 4. Calculated Mineral Modes of Fremdlinge (wt. %)

	F1	F2	F4	F5	F6	F9	F10	F11	F12	Zorba
NiFe metal	---	---	17.9	---	8.6	38.7	1.6	---	74.4	34.6
PtIr RMN	1.3	---	---	---	---	---	---	---	---	---
OsRu RMN	0.49	0.78	1.0	0.01	0.08	1.7	---	0.44	3.3	2.9
Magnetite	22.2	5.5	7.0	1.4	0.66	23.2	16.7	2.3	3.1	7.1
Pyrrhotite	27.3	---	---	79.2	80.8	3.1	32.3	76.8	---	21.9
Pentlandite	34.8	78.4	60.6	15.7	---	21.5	45.1	13.0	8.6	22.1
Molybdenite	3.5	1.3	2.1	0.02	0.17	3.1	---	0.11	0.61	7.4
Whitlockite	---	---	4.5	---	---	3.2	---	---	---	---
Fe-Silicate	6.2	14.0	6.9	1.8	4.8	5.5	1.0	4.6	5.0	1.5
Apatite	4.2	---	---	1.8	4.8	---	3.3	2.8	5.0	2.5
Attached silicates (as % of total sample)										
Fassaite	25.7	---	---	---	---	---	---	---	---	---
Melilite	40.3	---	---	---	---	---	---	---	---	---
Nepheline	---	---	---	10	---	---	10	---	---	---

silicate, seen to be minor phases, and 7% magnetite, compared to 3% by SEM. In F9, calculated proportions are 39% NiFe, 23% magnetite, 22% pentlandite, and 3% pyrrhotite. Both fragments of F9 studied by SEM contained only minor magnetite, and one contained major pyrrhotite. In F10, we calculate 45% pentlandite, 32% pyrrhotite, and 2% NiFe metal, compared to SEM estimates of 47, 17, and 17% of these phases, respectively. Proportions of calculated (17%) and observed (15%) magnetite are similar. Discrepancies in mineral proportions for these three inclusions are probably due to unrepresentative sections, particularly for F9 whose sections contain only the two largest fragments of the several studied by INAA.

For reasons stated above, we have neglected V-rich spinel. The maximum amount of this phase that could be present is estimated by calculating the maximum masses of additional Mg, Al, and O required by V-rich spinel such that the known sample masses are not exceeded beyond their errors. For F1, the sample with the smallest uncertainty in mass and the only sample in which V-rich spinel was observed by SEM, this estimate is $\leq 10\%$.

Bulk Compositions of Fremdlinge

The calculated, attached silicate-free weights of the ten opaque assemblages are listed in Table 5. Also shown are our best estimates of the bulk Fremdling compositions derived from these weights. Refractory siderophile element concentrations are normalized to their concentrations in C1 chondrites (ANDERS and GREVESSE, 1989) and plotted in order of decreasing condensation temperature (see below) in Fig. 1. Refractory siderophiles are strongly enriched relative to chondrites, some by a factor of $\geq 10^4$. Even sample F5, which has anomalously low concentrations of these elements compared to the other Fremdlinge, is enriched in them by factors of 10 to more than 100.

Sample F2 has the simplest pattern in Fig. 1, with enrichment factors rising smoothly from $5\text{–}6 \times 10^3$ for W and Re to $8\text{–}9 \times 10^3$ for Pt and Rh. All of the other samples contain large W anomalies. Only F5 has a positive W anomaly, with a C1 chondrite-normalized W/Re ratio of 3.7 ± 0.5. Negative anomalies exist in all remaining samples, with chondrite-normalized W/Re ratios varying from 0.48 ± 0.01 for F1 to $5.8 \pm 1.1 \times 10^{-3}$ for F4 and most samples having ratios of $\sim 10^{-2}$. In F6, a small negative W anomaly is superimposed on an irregular pattern of slightly rising enrichment factors with increasing volatility. Many samples also have large Mo anomalies. Three with negative W anomalies, F10, F11, and F12, also have negative Mo anomalies, with C1 chondrite-normalized Mo/Ir ratios ranging from 0.16 ± 0.02 for F11 to <0.10 for F10. In F12, these anomalies are superimposed on a pattern of steadily declining enrichment factors with increasing volatility, from 2.9×10^4 for Re and 3.5×10^4 for Os to 2.0×10^4 for Pt and Rh. For F10 and F11, large fractionations among the refractory siderophiles other than W and Mo show no regular relationship with volatility. Four with negative W anomalies, F1, F4, F9, and Zorba, have positive Mo anomalies, with chondrite-normalized Mo/Ir ratios ranging from 1.29 ± 0.05 in F4 to 5.8 ± 0.2 in F1. In these samples, enrichment factors for the more volatile siderophiles, Ru, Pt, and Rh, tend to be lower than those for the more refractory ones, Re, Os, and Ir, by amounts ranging from 15–20% in F1 to ~70% for Zorba. Large fractionations of W and Mo from other refractory siderophiles are clearly visible in Fig. 1, but its logarithmic scales tend to hide significant fractionations among siderophiles other than W and Mo. For example, C1 chondrite-normalized Re/Os, Os/Ru, Ir/Pt, and Pt/Rh range from 0.81–1.03, 0.67–3.32, 0.70–>2.25, and 0.45–1.43, respectively.

Table 5. Element Concentrations in Fremdlinge Recalculated on an Attached Silicate-free Basis

	mass(μg)	Fe(%)	Ni(%)	Ti(%)	V(%)	Cr(%)	Mn(%)	O(%)	Na(%)	Mg(%)	Al(%)	Si(%)	P(%)	S(%)	Ca(%)
F1	5.3	42.59	7.59	---	5.17	2.06	0.0198	10.6	< 0.15	0.85	0.65	1.0	0.78	22.9	3.00
F2	1.44	42.3	14.04	0.03	1.14	1.559	0.109	6.8	< 0.050	1.3	0.13	2.2	---	24.9	3.2
F4	2.8	36.7	23.5	0.04	0.987	0.850	0.0442	6.4	< 0.10	0.80	0.21	1.1	0.86	20.6	3.0
F5	0.65	56.3	3.50	0.003	0.118	0.29	2.61	1.8	---	0.17	0.03	0.30	0.34	35.0	1.14
F6	1.90	53.14	5.50	0.003	0.0976	0.23	0.729	4.0	< 0.095	0.44	0.02	0.79	0.92	30.4	3.00
F9	10.5	35.5	30.9	0.05	1.96	2.07	0.00208	9.3	< 0.051	0.78	0.50	0.94	0.54	9.4	2.1
F10	1.26	47.3	11.0	0.07	2.46	1.295	0.0088	6.5	---	0.27	0.43	0.15	0.62	27.1	1.5
F11	2.2	54.4	2.93	0.009	0.336	0.556	0.0139	3.5	< 0.09	0.44	0.06	0.74	0.52	33.1	2.14
F12	0.17	28.8	48.9	0.006	0.26	2.25	0.0407	4.5	< 0.78	0.45	0.07	0.76	0.90	3.1	3.0
Zorba	19.2	37.0	27.6	0.05	0.827	0.57	0.0028	3.6	0.042	0.18	0.14	0.25	0.44	18.7	1.32
C1 [1]		19.04	1.1		0.00565	0.266	0.1990								

	Sc	Co	Ta	W	Re	Os	Ir	Mo	Ru	Pt	Rh	Au	As	Sb	Se
F1	739.7	5278	< 0.53	219	180	2390	1870	21000	3070	3960	502	110.5	8.53	< 1.1	77.8
F2	25.1	6300	< 0.74	443	211	3371	3180	7840	5560	9290	1110	21.5	12.9	< 1.1	176
F4	4.07	6230	< 0.72	5.1	348	5520	4800	12000	4700	7730	1100	226.8	50	< 1.1	100
F5	0.73	536	< 0.56	30.6	3.24	51.3	15.6	133	110	< 15	---	1.70	< 5.9	5.5	< 7.0
F6	4.61	2190	< 0.37	34.5	36.3	580.4	650.9	995	708	1530	250	15.4	< 1.8	< 0.61	39.2
F9	7.17	7630	< 1.0	14.2	496	7710	7000	18200	5000	9900	1510	318	15.0	< 1.1	35
F10	10.3	4800	< 0.60	< 5.5	185	2393	1265	< 250	2780	1310	390	26.04	< 4.9	< 0.91	52.3
F11	4.55	1390	0.398	10.0	130	2137	2181	660	2090	4920	465	145.8	42.0	0.955	62.8
F12	< 2.2	22100	98.4	< 26	1070	17200	16200	3500	19200	19700	2720	1280	925	< 6.9	< 180
Zorba	5.2	7530	---	< 200	781	12700	14600	42400	5600	---	---	560	< 75	< 4.5	810
C1 [1]		502		0.0926	0.0365	0.486	0.481	0.928	0.712	0.990	0.134	0.140	1.86	0.142	18.6

Note: All units in ppm unless otherwise indicated. [1] C1 chondrite data from Anders and Grevesse (1989).

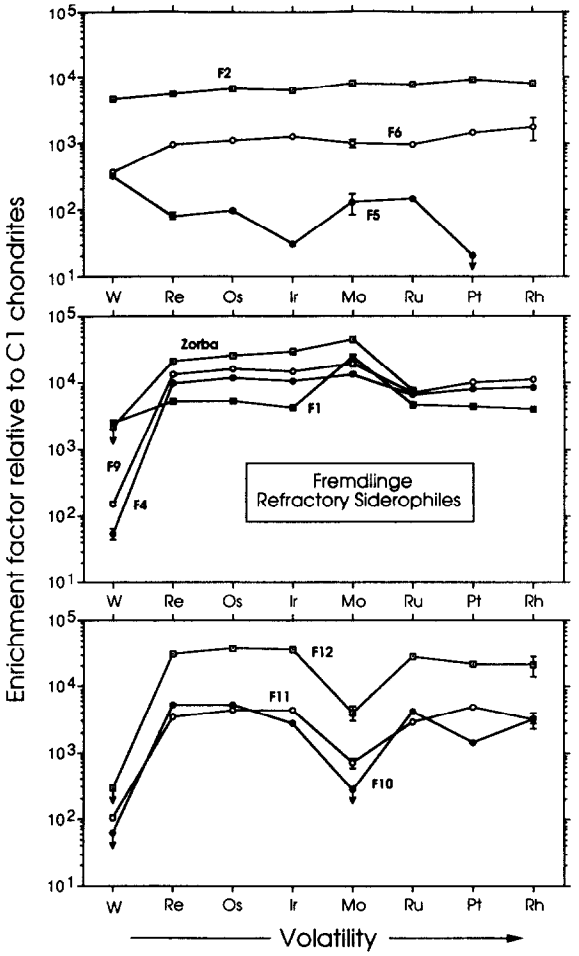

FIG. 1. Enrichment factors for refractory siderophiles in Fremdlinge relative to C1 chondrites, plotted in order of increasing volatility. 1σ error bars are shown when they are larger than the symbols.

Refractory siderophiles in seven Fremdlinge from Egg 6 previously reported by PALME et al. (1989) also have enrichment factors of 10^4 or more relative to C1 chondrites. All of these have large depletions of W compared to other siderophiles relative to C1 chondrites, and, like our samples, some of the PALME et al. (1989) samples also contain excesses or depletions of Mo compared to other siderophiles. Sample E2 of PALME et al. (1989) is similar to our samples F10 and F12 in having W and Mo depletions and lower enrichment factors on average for Ru, Pt, and Rh than for Re, Os, and Ir. Also, sample Florence of PALME et al. (1989) is similar to our sample F1 in having a W depletion and Mo excess, but differs in having a higher, rather than lower, mean enrichment factor for Ru and Pt than for Re, Os, and Ir. Several of the samples of PALME et al. (1989), E1, E4, and E6, show a progressive and rather steep decline in enrichment factor with increasing volatility which is not seen in any of our samples, although, in our work, F4, F9, and F10 have substantially lower mean enrichment factors for Ru, Pt, and Rh than for Re, Os, and Ir. Also, our sample F12 shows a progressive, but much less marked, decline in enrichment factor with volatility than E1, E4, and E6 and, in this way, is quite similar to sample Zelda of PALME et al. (1989). Refractory siderophile elements other than W and Mo are fractionated strongly from one another in the Fremdlinge studied by PALME et al. (1989), like in our samples, with chondrite-normalized Re/Os, Os/Ru, Ir/Pt, W/Re, and Mo/Ir ratios ranging from 0.82–1.05, 1.0–4.6, 0.87–5.3, <0.008–0.40, and <0.04–1.40, respectively.

Three Fremdlinge in our work are quite different from those of PALME et al. (1989). These include samples F2 and F6, which have progressively increasing enrichment factors with increasing volatility, and sample F5, which is strongly depleted in Ir and Pt relative to Re, Os, and Ru, compared to C1 chondrites. Also, F2 has no W anomaly and F5 a W excess, quite unlike all of the PALME et al. (1989) samples.

C1 chondrite-normalized enrichment factors for moderately volatile elements are plotted in Fig. 2 in the order of volatility (PALME et al., 1988). They tend to be less ($\leq 10^2$) than those for refractory siderophiles ($\geq 10^3$). Gold has enrichment factors intermediate between those of refractory siderophiles and those of other moderately volatile elements. C1 chondrite-normalized Ir/Au and Ni/Au ratios range from 2.7–43 and 0.002–0.26, respectively. Similar features were found in the Fremdlinge studied by PALME et al. (1989), except that ranges of Ir/Au and Ni/Au ratios are narrower in their samples due to less variation in Au. Even excepting Au, our samples do not show progressive trends in enrichment

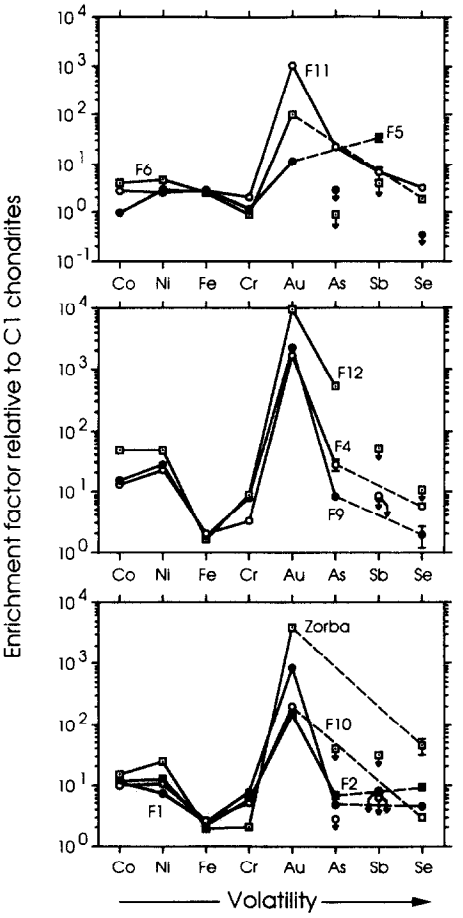

FIG. 2. Enrichment factors relative to C1 chondrites for moderately volatile elements in Fremdlinge, plotted in order of increasing volatility. Error bars as in Fig. 1.

factors from Co, the most refractory of these elements, to Se, the most volatile. F11, however, has higher enrichment factors for all three of the most volatile of these elements, As, Sb, and Se, than for the most refractory ones, Co, Ni, and Fe. Pairs of elements with similar condensation temperatures have C1 chondrite-normalized ratios which are highly variable in our samples. For example, the Fe/Ni ratio is usually subchondritic, varying from 0.03–0.56, except for F5 and F11 in which it is 0.93 and 1.07, respectively. The Co/Ni ratio is close to chondritic, 0.95–1.04, for four samples, but the total range is 0.34–1.52. Fremdlinge studied by PALME et al. (1989) have similar ranges of Fe/Ni and Co/Ni ratios. C1 chondrite-normalized As/Se ratios range from <0.47 to >52 in our samples.

DISCUSSION

Condensation of Refractory Siderophiles

Thermodynamic calculations were used to model the manner in which both refractory and volatile (Co, Ni, Fe, Cr, Au) siderophiles condense from a solar gas. In the calculations, it is assumed that, in a high-temperature gas of solar composition, the monatomic species is the only gaseous species for each of these elements, except W and Mo. For each of W and Mo, a term is also included for the gaseous monoxide. Abundances of the elements are taken from ANDERS and GREVESSE (1989), and the total pressure is assumed to be 10^{-3} atm. Thermodynamic data for most monatomic gaseous siderophile elements were taken from HULTGREN et al. (1973) and for $O_{(g)}$, $W_{(g)}$, $WO_{(g)}$, $Mo_{(g)}$, and $MoO_{(g)}$ from the JANAF Tables (CHASE et al., 1985). The partial pressure of oxygen as a function of temperature was taken from the full equilibrium calculations used for modeling condensation from a solar gas by LATTIMER and GROSSMAN (1978) in the temperature range 1700–2000 K. Compositions of condensate alloys are determined as a function of temperature, following calculations described in some detail previously (GROSSMAN, 1972; GROSSMAN and OLSEN, 1974; PALME and WLOTZKA, 1976; FEGLEY and PALME, 1985).

Our calculations examine two cases. The first assumes, as in all previous treatments of the subject (PALME and WLOTZKA, 1976; BLANDER et al., 1980; FEGLEY and PALME, 1985), that all refractory siderophiles form ideal solid solutions with each other, i.e., they condense into a common metal alloy. In this case, the mole fraction of an element in a condensate alloy equals the activity of that element because the activity coefficient is one. This is certainly an oversimplification, as phase separation is known to occur in the phase relations along many of the binaries between pairs of elements in this system.

The second model assumes that only those siderophiles with the same crystal structures at high temperatures form ideal solid solutions with each other. Thus, W, Mo, and Cr form a body-centered cubic (bcc) alloy; Re, Os, and Ru form a hexagonal close-packed (hcp) alloy, and Ir, Pt, Rh, Co, Ni, Fe, and Au form a face-centered cubic (fcc) alloy (BARRETT and MASSALSKI, 1980). The three phase model assumes that refractory siderophiles with different crystal structures are completely insoluble in one another; i.e., their activity coefficients are very large in one another, so their mole fractions approach zero in one another. These assumptions are not entirely correct, and the three phase model is, thus, also an oversimplification. Calculation of the precise behavior of these elements during condensation, however, would require a detailed knowledge of the variation with composition and temperature of the activity coefficient of each metal in all possible alloys containing the other 12 elements. Vastly more data are required than actually exist at present. That the three phase model is probably a more accurate description of the actual situation than the one phase model is suggested by the following data. Complete binary solid solutions, indicative of ideal solution behavior, are exhibited between all pairs of isostructural refractory siderophiles from the liquidus down to at least 2700°C for Re-Os, ~1000°C for Ir-Pt, ~850°C for Ir-Rh, ~800°C for Pt-Rh, at least 750°C for Re-Ru, and at all temperatures below the liquidus for W-Mo and Os-Ru (TYLKINA and SAVITSKII, 1978; BERLINCOURT et al., 1981; MASSALSKI, 1986). On the other hand, the binary phase relations for all pairs of refractory siderophiles with different, high-temperature crystal structures from one another, e.g., W-Re, Mo-Ir, and Pt-Ru, exhibit miscibility gaps, compound formation, and only limited solubility, even at their solidus temperatures (MASSALSKI, 1986), indicating non-ideal solution behavior at very high temperatures. There is a high probability of even greater deviations from ideality in alloys containing more than two elements, the likely situation during nebular condensation. In this discussion, we have ignored non-ideal effects involving Fe, Co, Cr, Ni, and Au, as these elements begin to condense significantly into these alloys at such low temperatures that all refractory siderophiles are already totally condensed. Possible effects of alloy formation between non-isostructural refractory siderophiles are discussed qualitatively later.

Figure 3 summarizes the results of the calculation assuming condensation of all refractory siderophiles into a common alloy. The condensed fraction of each element is plotted as a function of temperature. The results of this calculation are not significantly different from those of previous workers (PALME and WLOTZKA, 1976; BLANDER et al., 1980; FEGLEY and PALME, 1985). The alloy begins to condense at 1930 K. Re, Os, and W are the first siderophiles to condense from a cooling solar gas, followed by Ir, Mo, and Ru at significantly lower temperatures and then, at even lower temperatures, Pt and Rh. Note that all refractory siderophile elements are

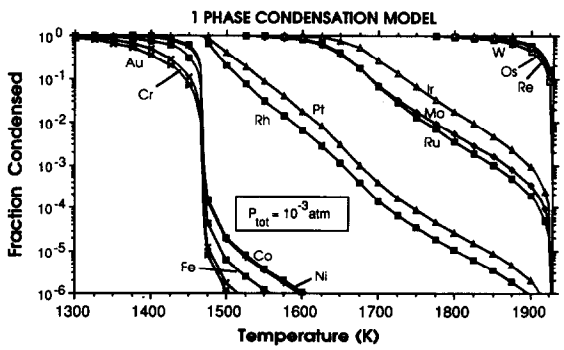

FIG. 3. Condensation curves for 13 siderophile elements condensing into a common alloy.

completely or almost completely condensed before a significant fraction of the Fe condenses at about 1460 K. Thus, fractionations between refractory siderophiles that are the result of condensation reflect processes occurring above this temperature and before large-scale condensation of Fe.

In both models, the activity of each metal is calculated at successively lower temperatures. In the three phase model, the condensation temperature of each alloy is the temperature at which the sum of the activities of the metals with the same crystal structure reaches one. Results of the three phase condensation model are shown in Fig. 4. The hcp alloy, consisting initially of ~90 atom% Os and 10% Re, appears at ~1925 K. The bcc alloy, consisting initially of ~99 atom% W and 1% Mo, appears at ~1810 K. The fcc alloy, consisting initially of ~97 atom% Ir and 3% Fe, appears at ~1645 K. Thus, there are some important differences in the order of condensation between the one phase and three phase models. In the three phase model, the onset of W and Mo condensation is delayed until the appearance of the bcc alloy and the onset of Ir, Pt, and Rh condensation until the appearance of the fcc alloy. In contrast to the one phase model, this causes Ru, which is in the hcp alloy, to condense at a higher temperature than Mo. Also, both Ru and Mo begin condensing well above the initial condensation temperature of Ir, but, since Ir has such a steep condensation curve, it is completely condensed at a slightly higher temperature than Ru and Mo.

In the next sections, we attempt to understand the compositions of Fremdlinge studied here in terms of both the one phase and three phase models. No attempt is made, however, to explain W and Mo concentrations by condensation models. PALME et al. (1989) found that, relative to C1 chondrites, W is depleted relative to other refractory siderophiles in Fremdlinge from Egg 6 and that some samples of the bulk inclusion are enriched in W relative to other siderophiles. Therefore, PALME et al. (1989) suggested that W was lost from Fremdlinge and deposited in the adjacent silicates during metamorphic oxidation and sulfidation. This suggestion finds some support in the experiments of KÖHLER et al. (1988) who found that W and Mo are preferentially removed from refractory metal grains when heated to 1200°C at the Ni/NiO buffer.

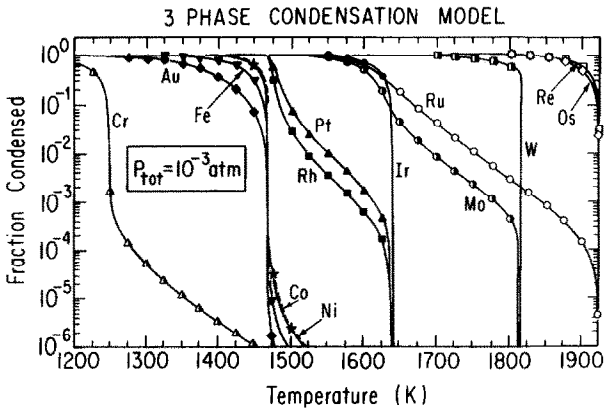

FIG. 4. Condensation curves for 13 siderophile elements condensing into bcc, hcp, and fcc alloys, as described in the text. Elements assumed to condense into the bcc alloy are indicated by half-filled symbols, into the hcp alloy by open symbols, and into the fcc alloy by filled symbols.

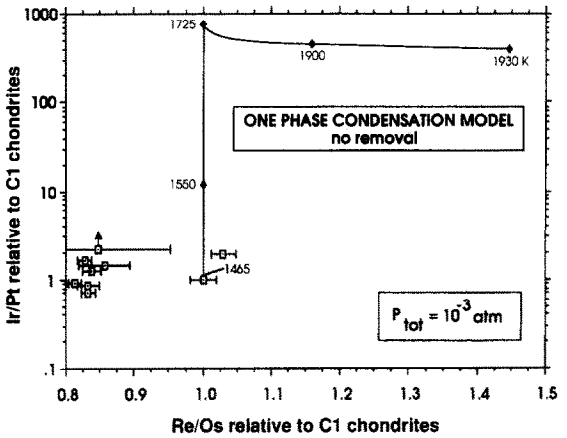

FIG. 5. C1 chondrite-normalized Ir/Pt vs. Re/Os ratios in the Fremdlinge studied here compared to ratios predicted in the one phase condensation model, assuming no removal of early condensates. Zorba is not plotted because its Pt concentration was not measured. Measured values are indicated by symbols with error bars. Model equilibration temperatures are indicated by diamonds. Error bars as in Fig. 1.

One Phase Condensation Model

Figure 5 shows the calculated condensation path for the one phase model on a plot of C1 chondrite-normalized Ir/Pt vs. Re/Os. The Ir/Pt ratio is much greater than one at high temperature (e.g., 400 at 1930 K) and increases slowly with decreasing temperature to a high of 750 at 1725 K. This is because Ir is much more refractory than Pt in a solar gas. This means that, at high temperature, the fraction of Ir condensed is several orders of magnitude greater and increases more rapidly with falling temperature than that of Pt (Fig. 3). At 1725 K, the Ir/Pt ratio of the condensate alloy begins to fall slowly with temperature. This reflects the fact that, below 1725 K, the rate of increase of the fraction of Pt condensed with falling temperature rises above that of Ir whose own rate slows below 1675 K as Ir nears the limit of total condensation. The ratio reaches one at 1465 K, where Pt reaches total condensation. In contrast to the Ir/Pt ratio, the Re/Os ratio is only slightly greater than one at high temperature (e.g., 1.45 at 1930 K), because Re is only slightly more refractory than Os. Since the condensation curve for Os is steeper than that for Re, the Re/Os ratio decreases with decreasing temperature, reaching one at 1725 K when both Re and Os are fully condensed.

Fremdling compositions from this work are also shown in Fig. 5. Eight samples have Re/Os ratios ~17% less than the chondritic value. Three samples also have subchondritic Ir/Pt ratios, from 0.70 to 0.91 relative to C1 chondrites. In contrast, Re/Os and Ir/Pt ratios are never less than the chondritic ratios in the one phase condensation model. We also investigated a one phase fractional condensation model in an attempt to explain Fremdling compositions. Since high-temperature alloys have Re/Os ratios greater than the chondritic ratio, removal of such alloys from the gas can cause lower

temperature alloys to have Re/Os ratios less than the chondritic value. Removal at 1905 K, for example, yields alloys with C1 chondrite-normalized Re/Os ratios of ~0.83, as in most of the Fremdlinge (Fig. 6). At 1905 K, however, insignificant Ir will have condensed, so that subsequently condensing alloys will never have subchondritic Ir/Pt ratios. A second fractionation that depletes the gas in Ir relative to Pt will yield subsequently condensing alloys with subchondritic Ir/Pt ratios, but they will contain almost no W, Re, and Os. This is because the latter elements are fully condensed before a significant fraction of the Ir condenses and will, thus, be removed with the Ir.

The one phase fractional condensation model also fails to explain other siderophile element ratios in Fremdlinge. For example, C1 chondrite-normalized Os/Ru ratios are between 1 and 2 in most Fremdlinge, whereas the model predicts values less than one, when a high-temperature alloy is removed (Fig. 7). This is because Os, which is much more refractory than Ru, is depleted relative to Ru during the 1905 K fractionation event required to explain the Re/Os ratios. In addition, at least one Fremdling has a subchondritic Pt/Rh ratio, which is not predicted by the one phase model (Fig. 7). These

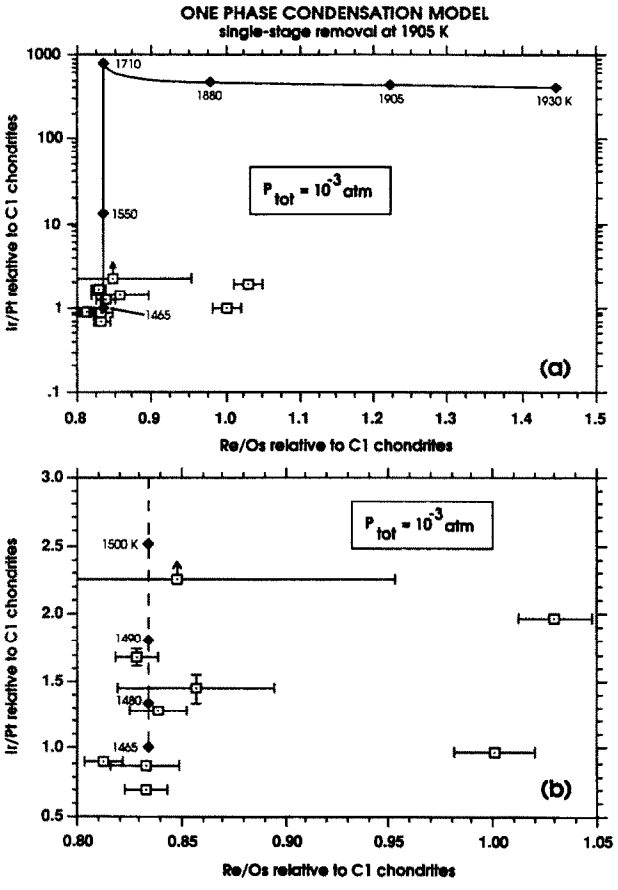

FIG. 6. (a) C1 chondrite-normalized Ir/Pt vs. Re/Os ratios in Fremdlinge compared to ratios predicted in the one phase condensation model, assuming removal of early condensates at 1905 K. Zorba is not plotted because its Pt concentration was not measured. (b) Close-up view of (a), in the region of the measured data. Note change from logarithmic to linear scale on *y*-axis. Symbols as in Fig. 5. Error bars as in Fig. 1.

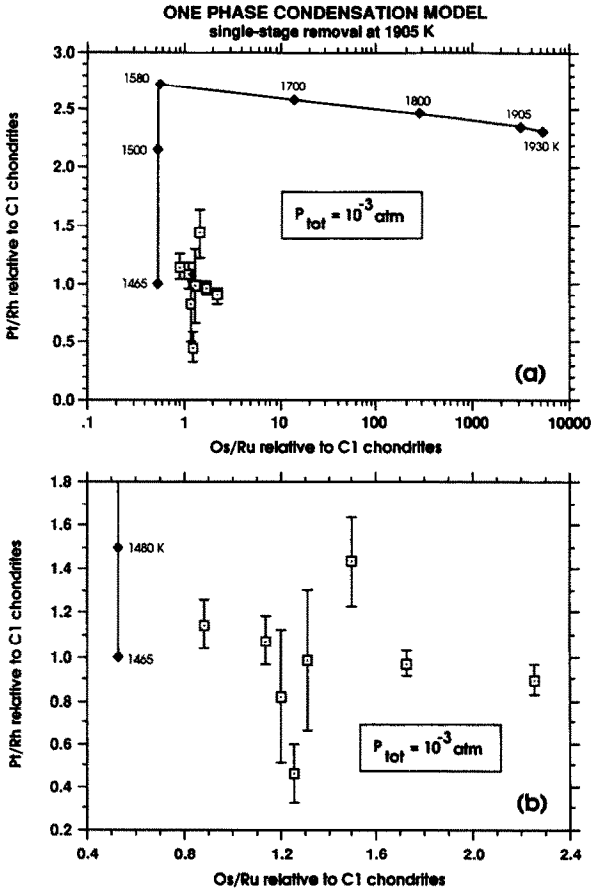

FIG. 7. (a) C1 chondrite-normalized Pt/Rh vs. Os/Ru ratios in Fremdlinge compared to ratios predicted in the one phase condensation model, assuming removal of early condensates at 1905 K. F5 and Zorba are not plotted because their Pt/Rh ratios are not known. (b) Close-up view of (a), in the region of the measured data. Note change from logarithmic to linear scale on *x*-axis. Symbols as in Fig. 5. Error bars as in Fig. 1.

relationships are not altered at lower pressure. At total pressures as low as 10^{-5} atm, one phase fractional condensation models are completely incapable of producing subchondritic Re/Os and Ir/Pt ratios and superchondritic Os/Ru ratios at a single temperature.

The above arguments assume that subchondritic Re/Os ratios observed in Fremdlinge are the result of condensation, as opposed to later metamorphism under oxidizing conditions. Since the latter process is probably responsible for the observed W and Mo depletions and FEGLEY and PALME (1985) suggest that Re is the next most oxidizable refractory siderophile, is it possible that Re, too, was lost from Fremdlinge during metamorphic oxidation? We think not because, while W and Mo sulfides are seen commonly in Fremdlinge, oxides and sulfides of Re are rare (EL GORESY et al., 1978). The single reported occurrence of high Re in oxide and sulfide phases is in a Fremdling in a Vigarano CAI (CAILLET et al., 1988). Also, the correlation that would be expected between Re depletions and W and Mo depletions is not very good. For example, F5 and F2 have the usual C1 chondrite-normalized Re/Os ratio, 0.84 ± 0.10 and 0.83 ± 0.01, respectively, but F5 is actually enriched in W and Mo, with chon-

drite-normalized W/Os and Mo/Ir ratios of 3.1 ± 0.2 and 4.4 ± 0.5, respectively. F2 is only slightly depleted in W and enriched in Mo, with W/Os and Mo/Ir ratios of 0.69 ± 0.01 and 1.28 ± 0.01, respectively. Furthermore, F4, F9, and Zorba have W and Re depletions but also have Mo excesses. Finally, F10 is one of only two samples with a chondritic Re/Os ratio, 1.03 ± 0.02; yet, it has the lowest chondrite-normalized Mo/Ir ratio, <0.10, and one of the lowest W/Os ratios, <0.012.

The above arguments also assume that observed fractionations among refractory siderophiles are not the result of non-representative, laboratory sampling of minor Fremdling phases with diverse compositions. As seen above, Fremdlinge in Egg 6 have bulk Re/Os ratios which are either ~1.0 or ~0.83 relative to C1 chondrites. Non-representative sampling of minor phases with different Re/Os ratios would be expected to yield Fremdling compositions with both enrichments and depletions of Re relative to Os compared to C1 chondrites and by variable amounts.

It is also possible that current best estimates of the siderophile abundances in C1 chondrites (ANDERS and GREVESSE, 1989) are in error such that the Fremdlinge do not have subchondritic Re/Os, Ir/Pt, and Pt/Rh ratios. Even if the cosmic abundance ratios for these element pairs are reduced to the lowest values in Fremdlinge, however, a condensation curve analogous to that in Fig. 5 that intersects the cluster of Fremdlinge will not intersect F1 and F10, whose Re/Os ratios are significantly higher. In this case, if an alloy is removed at high temperature and is subsequently added to low-temperature condensates, the mixture could have a higher Re/Os ratio than low-temperature alloys that escaped this remixing. Such a mixture, however, would also have the highest Os/Ru ratio, which is not the case for either F1 or F10. Because we have not investigated condensation from gases of non-solar composition, we cannot rule out the possibility that all of the observed element fractionations in Fremdlinge could be produced during condensation of a single alloy phase from such a gas.

Three Phase Condensation Model

In the three phase model, bcc, hcp, and fcc alloys condense from a gas of solar composition and subsequently accumulate to form proto-Fremdlinge. Mixing of the three alloys occurs either in the nebular gas, before and during accumulation of the major oxide and silicate phases into CAIs, or in CAIs themselves, when the latter phases, as well as the alloys, were subsequently partially melted. PALME and WLOTZKA (1976) calculated that it would take 500–5000 years to grow a Fremdling-sized (~10 μm) particle from the nebular gas. Such long time scales are unnecessary if, as envisaged here, the actual condensate grains were submicron-sized and only formed Fremdling-sized particles during later accretion and melting processes. As pointed out by BLUM et al. (1989), Fe-rich alloys, such as the fcc condensate alloy discussed herein, are expected to be molten at the temperatures of CAI melting. Although hcp and bcc condensate alloys have higher melting points due to their anticipated lower Fe contents, they, too, would have become molten by dissolving in the Fe-rich droplets immediately upon contact with them. The final stage in the production of Fremdlinge occurs when oxygen and sulfur are added to the proto-Fremdlinge at relatively low temperatures (BLUM et al., 1989).

For the hcp alloy (Fig. 8), continuous removal of high-temperature condensates until the temperature falls to 1907 K yields subsequent, lower-temperature (≤1750 K) condensates with C1 chondrite-normalized Re/Os ratios of about 0.83, as is observed in most Fremdlinge. The subsequently condensing alloys must equilibrate at temperatures ranging from 1638 K to 1530 K to form proto-Fremdlinge with Os/Ru ratios from slightly greater than three to slightly less than one relative to C1 chondrites. Two Fremdlinge with approximately chondritic Re/Os and Os/Ru ratios may have accumulated from constituents that did not undergo this high-temperature fractionation event. Alternatively, they may have formed by mixing ~8.5 parts of a condensate that equilibrated at 1555 K with 1 part of the previously removed, high temperature alloy.

It is not possible to apply the condensation model to the W/Mo ratios of these samples because W, and possibly also Mo, was probably leached from Fremdlinge during volatile alteration. We note, however, that total condensation of W and Mo in the bcc alloy that contributed to Fremdlinge would require low equilibration temperatures (~1465 K). For the fcc alloy (Fig. 9), Fremdling precursors with C1 chondrite-

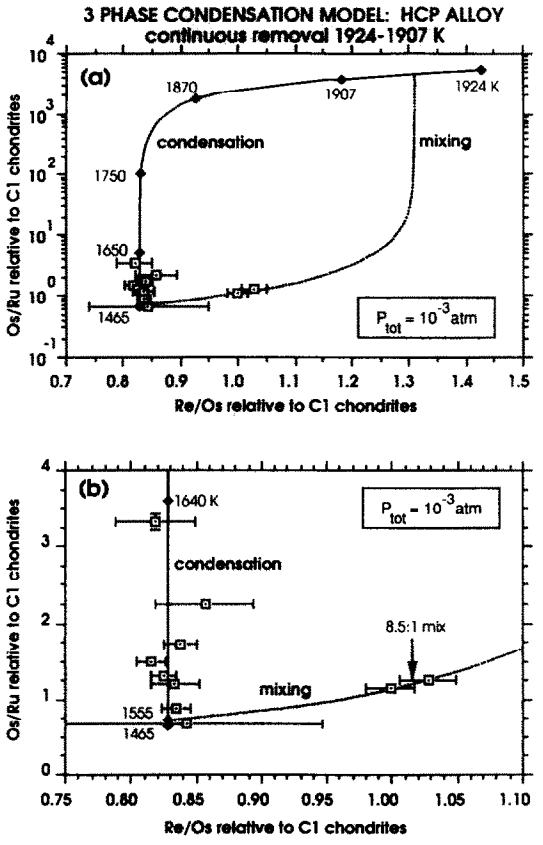

FIG. 8. (a) C1 chondrite-normalized Os/Ru vs. Re/Os ratios in Fremdlinge compared to ratios predicted in an hcp alloy by the three phase condensation model, assuming continuous removal of early condensates between 1924 and 1907 K. (b) Close-up view of (a), in the region of the measured data. Note change from logarithmic to linear scale on *y*-axis. Symbols as in Fig. 5. Error bars as in Fig. 1.

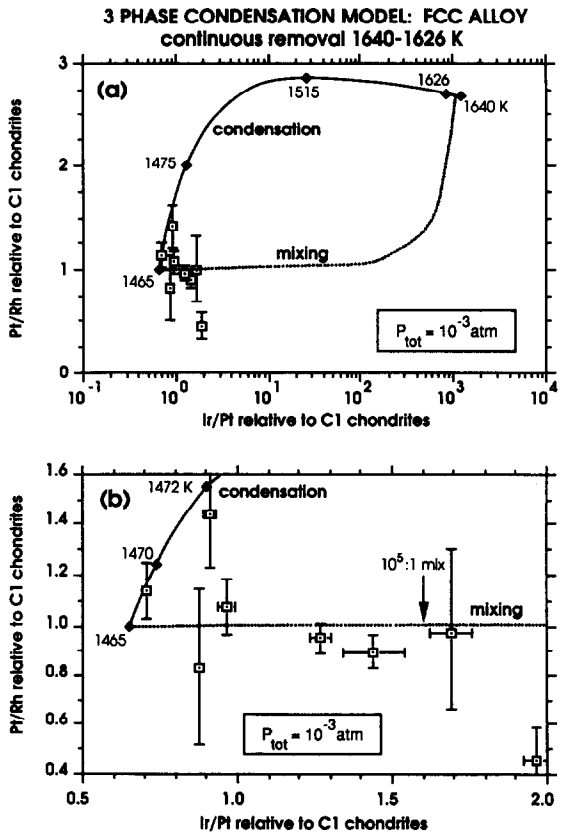

FIG. 9. (a) C1 chondrite-normalized Pt/Rh vs. Ir/Pt ratios in Fremdlinge compared to ratios predicted in an fcc alloy by the three phase condensation model, assuming continuous removal of early condensates between 1640 and 1626 K. (b) Close-up view of (a), in the region of the measured data. Note change from logarithmic to linear scale on x-axis. Symbols as in Fig. 5. Error bars as in Fig. 1.

normalized Ir/Pt ratios less than one are explained by continuous removal of high-temperature condensates until 1626 K. Alloys condensing from the fractionated gas equilibrate within a narrow temperature interval (1478–1465 K) to give proto-Fremdlinge with close to chondritic Pt/Rh ratios. In most samples, these low-temperature alloys must be mixed back with the removed condensate in varying proportions to explain Ir/Pt ratios that are greater than the C1 value. A Fremdling with a C1 chondrite-normalized Ir/Pt ratio of 1.6, for example, can be modelled by mixing $\sim 10^5$ parts of a condensate equilibrated at 1465 K with 1 part of the previously removed, high-temperature condensate.

At total pressures as low as 10^{-5} atm, Re is still more completely condensed than Os in the hcp alloy at a given temperature, and Ir is still more completely condensed than Pt in the fcc alloy at a given temperature. This means that fractional condensation is still required in order to produce subchondritic Re/Os and Ir/Pt ratios in the three phase model at pressures lower than 10^{-3} atm.

At least one Fremdling, F10, has a subchondritic Pt/Rh ratio, 0.45 ± 0.13, that is not explained by the above nebular history of the fcc alloy. Since Pt is only slightly more refractory than Rh, and less than one part in a thousand of the total Pt and Rh condense into the removed high-temperature fcc alloy, subsequent, low-temperature fcc condensates do not have subchondritic Pt/Rh ratios. If the three phase model is valid, another mechanism must be responsible for this low ratio. One possibility is condensation of some of the Pt and Rh in the hcp or bcc alloy. Unfortunately, the relative solubilities of Pt and Rh are not known in the most abundant elements in the hcp alloy, Ru and Os, or in the bcc alloy, Mo. If a larger fraction of the Pt than the Rh could form hcp or bcc alloys, the latter could condense from the nebular gas with C1 chondrite-normalized Pt/Rh ratios greater than one, and subsequent fcc alloys that condensed from the same gas could ultimately achieve ratios that are less than one. Mixing of relatively large amounts of the fcc alloy with relatively small amounts of the hcp alloy could, thus, form proto-Fremdlinge with subchondritic Pt/Rh ratios. Sample F10 does contain much more fcc alloy than hcp alloy (see below) but so do most other samples and none of these have subchondritic Pt/Rh ratios. This suggests that the solution of Pt and Rh in the hcp alloy was probably not responsible for the subchondritic Pt/Rh ratio in F10.

In Table 6 are shown the relative proportions and equilibration temperatures of condensate alloys required to match the refractory siderophile element enrichment pattern in each Fremdling. In cases requiring mixing of an early condensate removed at high temperature with a later-condensing, isostructural alloy, the table gives the temperature range over which the high-temperature phase was removed continuously. For the purpose of this table, the amount of bcc alloy was calculated by assuming that both W and Mo were fully condensed into it, i.e., it equilibrated with the nebular gas at 1465 K, and that Mo contents of Fremdlinge were unaffected by later alteration. For Zorba, it had to be assumed that the fcc alloy also equilibrated at 1465 K, because its Pt and Rh concentrations were not measured. These data were used to calculate model enrichment factors of refractory siderophiles relative to Os compared to C1 chondrites for all ten Fremdlinge. The data for five of these are plotted in Fig. 10, where they are compared to similarly normalized, measured data for the same Fremdlinge. Except for W, which is known to have been affected by volatile alteration (PALME et al., 1989), and the Pt/Rh ratio in F10, which was discussed above, the model abundances are within error of the observed abundances for each sample. The excellent degree of coherence between the model and observed patterns is to be expected

Table 6. Condensate Alloy Mixtures in Each Fremdling

	HCP Alloy		FCC Alloy		BCC Alloy	
Sample	T(K)	%	T(K)	%	T(K)	%
F1	1924-1907	0.0004	1640-1626	0.0003	1465	0.0248
	1555	0.0040	1465	99.97		
F2	1584	1.58	1470	96.44	1465	1.98
F4	1619	0.0037	1640-1626	0.0006	1465	0.0071
			1465	99.99		
F5	1530	35.84	> 1479	24.60	1465	39.56
F6	1604	0.0026	1640-1626	0.0002	1465	0.0030
			1465	99.99		
F9	1627	0.0036	1640-1626	0.0008	1465	0.0085
			1465	99.99		
F10	1924-1907	0.0014	1640-1626	0.0013	1465	0.0009
	1555	0.0107	1465	99.98		
F11	1614	4.19	1472	94.77	1465	1.04
F12	1608	0.0057	1640-1626	0.0011	1465	0.0009
			1465	99.99		
Zorba	1638	0.0010	1465	99.99	1465	0.0043

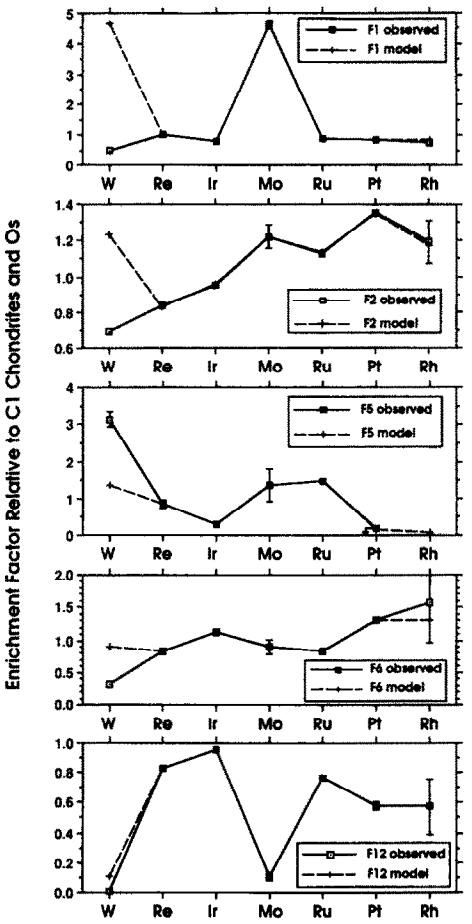

FIG. 10. Comparison between enrichment factors for refractory siderophiles relative to C1 chondrites and Os in five Fremdlinge, and those predicted by the three phase condensation model. Error bars as in Fig. 1.

from the large number of free parameters in the three phase model, which are not available in the one phase model.

Except for F5, the fcc alloy is the most abundant of the three alloys (>94%) in each Fremdling. Relative proportions of hcp and bcc alloys range from 0.001–4.2% and 0.0008–2.0%, respectively. In F5, the proportions are 24% fcc alloy, 36% hcp alloy, and 40% bcc alloy. The reason why the fcc alloy dominates is that Fe, which is much more abundant than refractory siderophiles, begins to condense significantly ($>10^{-5}$ of the total Fe) into the fcc alloy at ~1473 K and most proto-Fremdlinge accumulated from fcc alloys that equilibrated at slightly lower temperatures, 1472–1465 K. The fcc alloy that formed F5, however, equilibrated at ~1479 K, a temperature at which much less Fe had condensed. The relative proportions of the different alloys required to construct each proto-Fremdling are different from the relative proportions that are predicted to have existed in the solar nebula at the equilibration temperatures shown in Table 6. Relative to the nebular proportions, the ranges of fcc/hcp, bcc/hcp, and bcc/fcc ratios in Fremdlinge are 0.30–1.44, 0.03–2.33, and 0.04–3.0, respectively. The bcc/hcp and bcc/fcc ratios may be underestimates, as the amount of bcc alloy is based on Mo which, as noted earlier, may have been lost from Fremdlinge during secondary alteration. Fractionation of these alloys relative to one another in Fremdlinge compared to their nebular proportions may simply be the result of grain-gas separation processes in the nebula prior to and during aggregation of clumps of alloy grains and/or nonrepresentative sampling by immiscible alloy droplets in molten CAIs.

FEGLEY and PALME (1985) suggested that condensation from an oxidizing gas may be responsible for W and Mo depletions seen in some bulk CAIs and Fremdlinge but, in this case, larger depletions are predicted for Mo than W, as Mo is more volatile than W. This cannot be the explanation for W and Mo anomalies in the Egg 6 Fremdlinge since, in cases where both W and Mo are depleted, W depletions are always larger than Mo depletions. Furthermore, condensation from an oxidizing gas cannot readily explain the patterns of refractory siderophile enrichments found in F1, F9, and Zorba, which have Mo excesses. Both excesses and depletions of W and Mo relative to other refractory siderophiles can easily be produced in the three phase condensation model without appealing to oxidizing conditions. In such a model, such fractionations would simply be related to the equilibration temperature of the bcc alloy and the relative mixing proportions of bcc and other alloys. As discussed above, however, application of this model to W and Mo concentrations in Fremdlinge from Egg 6 is complicated by later loss of W and possibly also Mo during low-temperature oxidation and sulfidation. It is conceivable that some non-solar gas composition exists from which condensation of three phases could produce the entire range of element fractionations observed in Fremdlinge without removal of early condensates, but we have not conducted a search for such a composition.

Effects of Alloying between Non-Isostructural Metals

The three phase model assumes no solid solution between elements of different crystal structure. Although we do not have the data to model quantitatively the extent to which this assumption is violated, we can assess such behavior qualitatively from binary phase relations of refractory siderophiles. Of particular interest is the possibility that partial solubilities of non-isostructural metals in one another can cause fractionation of Re from Os or of Ir from Pt, as C1 chondrite-normalized Re/Os and Ir/Pt ratios less than one otherwise require separation of early, high-temperature condensate hcp and fcc alloys from the nebular gas.

In the case of Re and Os, the three phase model predicts total condensation of both elements in an hcp alloy before W begins to condense in a bcc alloy at ~1810 K (Fig. 4). At this temperature, the hcp alloy is ~93 atomic % Os and the bcc alloy is virtually 100% W. Assuming that the small amount of Ru in the hcp alloy and of Mo in the bcc alloy have little effect, the Os-W binary phase relations (MASSALSKI, 1986) may provide clues to the directions of deviations from the three phase condensation model. Because Os can dissolve 35 atomic % W at this temperature, a significant fraction of the W can probably condense in the hcp alloy above 1810 K. It seems unlikely that dissolution of W in Os could reduce the solubility of Re in Os sufficiently, however, to produce condensate alloys with subchondritic Re/Os ratios, as total condensation of Re into such an alloy requires a Re solubility of only ≤7%.

We now consider whether subchondritic Ir/Pt ratios, which lead us to fractional condensation of high-temperature, relatively Ir-rich, fcc alloys in the three phase model, may instead be due to solution of a greater fraction of the Ir than the Pt in higher temperature bcc or hcp alloys. Regardless of how much W condenses in the hcp alloy, the bcc alloy will be composed predominantly of Mo at 1644 K, where Ir otherwise begins to condense in the fcc alloy. Binary phase diagrams for the systems Ir-Mo and Pt-Mo (MASSALSKI, 1986) suggest that, at this temperature, ~7% Ir and ~5% Pt can dissolve in Mo. Neglecting the possible effect of W on the relative solubilities of Ir and Pt in this alloy, and the possible effect of Pt and Ir on each other's solubilities, this would be sufficient to reduce the C1 chondrite-normalized Ir/Pt ratio to ~0.82 in the fcc condensate alloy, a value approaching the lowest observed value in Fremdlinge, 0.70. At 1644 K, the hcp alloy is composed predominantly of Os and Ru. Although we do not know the relative solubilities of Ir and Pt in Os, binary phase diagrams for the systems Ir-Ru and Pt-Ru (MASSALSKI, 1986) show that ~42% Ir and ~62% Pt can dissolve in Ru at this temperature. This, too, would be sufficient to reduce the C1 chondrite-normalized Ir/Pt ratio in fcc condensate alloys, especially if Ir and Pt have similar solubilities in Os as in Ru. We can, therefore, not rule out the possibility that subchondritic Ir/Pt ratios in Fremdlinge are the result of partial solution of Ir and Pt in bcc and/or hcp alloys.

Origin of Volatile Elements

The three phase condensation model makes specific predictions about concentrations of volatile siderophile elements, Co, Ni, Fe, Au, and Cr, in condensate fcc and hcp alloys. In Fig. 11, C1 chondrite-normalized, volatile siderophile element/Ni ratios in representative Fremdlinge are compared to those calculated using the relative proportions of fcc and hcp alloys shown in Table 5. Iridium is included in order to compare relative abundances of refractory and volatile siderophiles.

In all samples except F2, F5, and F11, Ir/Ni ratios are significantly higher than predicted by the three phase model, 260-1210 vs. 4-12, respectively. High Ir/Ni ratios in these Fremdlinge could reflect either loss of Ni relative to Ir during metamorphic oxidation and sulfidation, or higher equilibration temperatures for the low-temperature fcc alloys, 1468–1469 K, than those predicted from Ir/Pt and Pt/Rh ratios, 1465 K. Except for F10, Ir/Pt and Pt/Rh ratios in these Fremdlinge have 2σ errors that allow equilibration of the low-temperature fcc alloy at 1468–1469 K. Conversely, in F2 and F5, which have lower C1-normalized Ir/Ni ratios, 520 and 10, respectively, than those predicted by the three phase model, 2060 and 56800, respectively, the 2σ errors on the Ir/Pt and Pt/Rh ratios allow low enough equilibration temperatures for the observed and model Ir/Ni ratios to agree. This is not the case for F11, however; this sample may have gained Ni relative to Ir during secondary alteration.

C1 chondrite-normalized Co/Ni ratios in all samples except F1 are lower than predicted by the three phase model, 0.34–1.04 vs. 1.08–1.10, respectively. This discrepancy cannot be a consequence of uncertainty in the precise equilibration

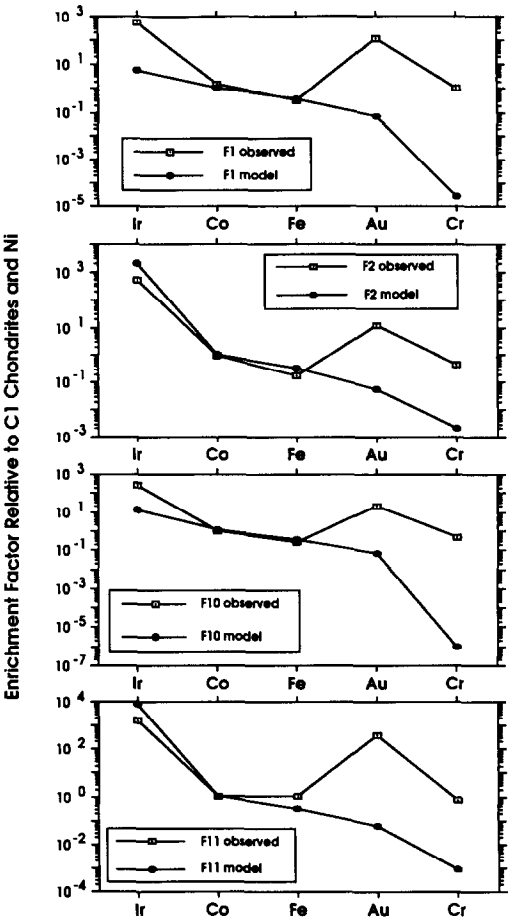

FIG. 11. Comparison between enrichment factors for Ir, Co, Fe, Au, and Cr relative to C1 chondrites and Ni in four Fremdlinge, and those predicted by the three phase condensation model. Error bars as in Fig. 1.

temperature of fcc alloys in Fremdlinge, since Co/Ni ratios of such alloys decrease only slightly from 1.14 at 1625 K to 1.06 at 1460 K. The ratio of 1.04, which is found in F11, is not reached until even lower temperatures, and subchondritic ratios, which are found in the other samples, are not achieved by condensation. Thus, after condensation, Co was probably lost relative to Ni in these Fremdlinge. In F1, however, the high Co/Ni ratio, 1.52, possibly reflects gain of Co relative to Ni.

C1 chondrite-normalized Fe/Ni ratios in all samples except F1, F5, F6, and F11 are lower than predicted by the three phase model, 0.03–0.25 vs. 0.32–0.36, respectively. Because Fe/Ni ratios in fcc condensate alloys do not fall below 0.32 at any equilibration temperature, these samples probably lost Fe relative to Ni during secondary alteration, as suggested previously (ARMSTRONG et al., 1987; BLUM et al., 1989). In contrast, the high C1-normalized Fe/Ni ratios in F5, F6, and F11, 0.93, 0.56, and 1.07, respectively, may reflect relative gain of Fe during secondary alteration. Only F1, whose ratio, 0.33, is similar to that predicted by the three phase model, 0.36, may have escaped Fe loss or gain after condensation.

C1 chondrite-normalized Au/Ni and Cr/Ni ratios are higher than predicted by the three phase model for all samples

by factors of 10^2–10^3 and 2–10^4, respectively. These large differences suggest that most of the Au and Cr in Fremdlinge was added during secondary oxidation and sulfidation and is not the result of primary condensation. As noted earlier, Au is anomalously enriched in Fremdlinge compared to volatile siderophile elements of both higher and lower condensation temperature (Fig. 2). If the more volatile siderophiles, As and Sb, and the more volatile chalcophile, Se, were also added during alteration, then they were not retained by Fremdlinge as well as was Au.

Physical Processes of Fremdling Formation

Chemical compositions of Egg 6 Fremdlinge suggest that they contain components which accumulated from hcp, bcc, and fcc alloys that condensed from the nebular gas. Removal of early, high-temperature hcp condensate alloys from the gas seems to be required to explain subchondritic Re/Os ratios found in many Fremdlinge. High-temperature fractionation of fcc condensate alloys may also be necessary to explain Fremdlinge with subchondritic Ir/Pt ratios.

Subchondritic Re/Os and Ir/Pt ratios in Fremdlinge are not the only chemical signatures that record early, high-temperature fractionation processes in the formation of CAIs. Group II REE patterns, found most commonly in the bulk compositions of fine-grained CAIs, also are thought to form after removal of a high-temperature, ultrarefractory condensate. In the latter case, however, the removed condensate contains the most refractory REE, i.e., the heavy ones except Tm and Yb (BOYNTON, 1975; DAVIS and GROSSMAN, 1979). Like Group II REE patterns, subchondritic Re/Os and Ir/Pt ratios in Fremdlinge are compelling evidence for the role of condensation in the formation of CAIs. CAIs or their constituents that possess either of these chemical signatures cannot be simple residues left over after evaporation of nebular solids (e.g., CHOU et al., 1976).

There are at least two processes by which high-temperature hcp and fcc condensate alloys could have been removed from chemical contact with the nebular gas: entrapment of the alloys in early condensing oxide phases and transport of the alloys to a region of the nebula from which refractory siderophiles had already condensed. It is unlikely that hcp alloys were entrapped in early oxide condensates, however. The removal temperatures of hcp alloys, 1924–1907 K, are significantly higher than the condensation temperature of corundum (1758 K at 10^{-3} atm; GROSSMAN, 1972), the earliest major oxide phase to condense. Early condensate fcc alloys, in contrast, were removed from the gas at much lower temperatures, 1640–1626 K, and, thus, could have become entrapped in oxide condensates. Transport of early condensate hcp and fcc alloys to another region of the nebula requires a mechanism capable of separating submicron-sized particles from the surrounding gas at high temperature. Whatever the mechanism, the existence of Fremdlinge with C1 chondrite-normalized Re/Os and Ir/Pt ratios greater than one requires that those early condensates be mixed back together with some of the proto-Fremdlinge.

Large fractionations between refractory siderophile elements in the Fremdlinge studied here are found neither in Egg 6, the CAI from which they were removed, nor in other coarse-grained Allende CAIs. C1 chondrite-normalized Re/Os, Os/Ru, Ir/Pt, and Os/Ir ratios are 0.81–1.03, 0.67–3.32, 0.70–>2.25, and 0.86–3.3, respectively, in the Fremdlinge, and 0.96, 1.1, 1.3, and 1.1, respectively, in Egg 6 (PALME et al., 1989). In individual, coarse-grained Allende CAIs, Re/Os, Os/Ru, and Os/Ir ratios are within 10–15% of C1 chondritic ratios (GROSSMAN and GANAPATHY, 1976; GROSSMAN et al., 1977). These observations suggest that each CAI contains such a large number of Fremdlinge that the excesses and depletions of some refractory siderophiles relative to others in individual Fremdlinge are largely cancelled out through mixing.

To pursue this idea, C1 chondrite-normalized, weighted average compositions for Fremdlinge and Egg 6 (PALME et al., 1989) are shown in Table 7. Data from PALME et al. (1989) for Zelda, the largest Fremdling, 504 μg, in Egg 6 are included in one weighted average. The weighted average Fremdling compositions have fractionations between Re, Os, Ir, Pt, and Rh that are smaller than those in individual Fremdlinge. As seen in Table 7, the C1 chondrite-normalized Re/Os and Os/Ir ratios, for example, are 1.00 and 1.09, respectively, in the weighted average composition that includes Zelda. In the nine Fremdling average, C1 chondrite-normalized Ir/Pt and Pt/Rh ratios are 1.29 and 0.94, respectively. Ruthenium, however, is almost as fractionated in the weighted average Fremdling compositions as it is in individual Fremdlinge. Osmium/ruthenium ratios are 1.7–2.6 times the C1 chondritic ratio in the three weighted average compositions. This is because the hcp alloy that carried Ru into most of the Fremdlinge stopped equilibrating with the nebular gas at a high enough temperature, 1650–1530 K, that Ru had not fully condensed into it (Fig. 8b and Table 6). Later condensing, Ru-enriched hcp alloys were apparently not incorporated into Fremdlinge. An alternative, that Ru was lost from Fremdlinge by S addition during metamorphism, is ruled out by the fact that RuS_2 cannot form under the f_{S_2}-T conditions that existed during metamorphism (BLUM et al., 1989) and that Ru is never found as a sulfide in Fremdlinge. Since the C1 chondrite-normalized Os/Ru ratio in Egg 6 is 1.1, this inclusion must contain most of the Ru missing from Fremdlinge, probably in a Ru-rich phase that we did not sample, perhaps because that phase occurs in grains separate

Table 7. Weighted Average Fremdling and Egg 6 Enrichment Factors Relative to C1 Chondrites

Element	9 Fremdlinge	9 Fremdlinge + Zorba	9 Fremdlinge + Zorba + Zelda	Egg 6
W	< 860	< 1400	< 190	32
Re	8580	14000	6190	27
Os	9870	16700	6180	28
Ir	8870	17900	5660	26
Mo	14500	27700	6930	21
Ru	5500	6500	3590	25
Pt	6890	---	---	20
Rh	7300	---	---	---
Au	1410	2510	588	---
Co	11.6	13.0	7.29	---
Ni	17.1	20.5	9.83	---
Fe	2.17	2.07	2.54	---
Cr	5.90	4.32	5.05	---
Ratios relative to C1				
Re/Os	0.87	0.84	1.00	0.96
Os/Ir	1.11	0.93	1.09	1.1
Ir/Pt	1.29	---	---	1.3
Pt/Rh	0.94	---	---	---
Os/Ru	1.79	2.57	1.72	1.1
Fraction of Egg 6	0.29 %	0.15 %	0.46 %	

Note: Data for Zelda and Egg 6 from Palme *et al.* (1989).

from and much smaller than Fremdlinge. Tiny, Ru-rich RMN, which have been identified in other CAIs (FUCHS and BLANDER, 1980; WARK, 1986; PAQUE, 1989), may, therefore, be important carriers of Ru in Egg 6. Such grains may be related to the late-condensing, Ru-rich alloys predicted to form above and may have escaped coalescence into Fremdlinge during partial melting of Type B inclusions by being trapped inside grains of phases which did not melt.

The weighted average compositions in Table 7 indicate that Fremdlinge constitute 0.15–0.46% of Egg 6, assuming that all Ir in Egg 6 is in Fremdlinge. Fremdlinge probably comprise only 0.09–0.30% of most coarse-grained Allende CAIs, however, since the latter are somewhat less enriched in refractory siderophiles, ~17 times C1 chondrites (GROSSMAN, 1980), than is Egg 6, ~26 times C1 chondrites. GROSSMAN and GANAPATHY (1976) measured the concentrations of Co, Fe, Cr, and Au in seven Allende Type B CAIs. If the latter contain Fremdlinge whose mean composition is the same as that found here for the weighted average that includes Zelda, then Fremdlinge contribute >52%, >16%, and >5% of the indigenous Co, Fe, and Cr, respectively, in the average inclusion. These are lower limits because measured concentrations of these elements in bulk CAIs include amounts due to matrix contamination during sampling in addition to the indigenous amounts of these elements. For Au, this calculation implies that Fremdlinge contribute 2.8 times more Au than is actually present in the average inclusion, suggesting that most of the Au in CAIs is in Fremdlinge.

CONCLUSION

Large fractionations between refractory siderophiles in individual Fremdlinge cannot be explained if all of these elements condensed from the solar nebula into a single phase. Fremdling compositions can be understood if these elements condensed into three separate alloys according to their crystal structures, if fractionated alloys were removed from chemical communication with the gas at high temperature, producing lower-temperature alloys with complementary fractionations, and if Fremdlinge formed by mixing of variable proportions of high- and low-temperature varieties of the three alloys. This mixing occurred by grain aggregation in the solar nebula, prior to and during accretion of CAIs, and by coalescence of droplets of immiscible metal-P liquids during later partial melting of CAIs, forming proto-Fremdlinge. Fremdlinge formed from these by still lower-temperature addition of oxygen, sulfur, and other volatiles, during which process W, and possibly also Mo, was mobilized, lost from Fremdlinge, and deposited into adjacent silicate and oxide phases in their CAI hosts.

Acknowledgments—We thank B. D. Keck for assistance with irradiations at the University of Missouri Research Reactor that went far beyond the normal call of duty, and L. Hedges for assistance with separating, mounting, and polishing the Fremdlinge. Helpful discussions with A. M. Davis, S. B. Simon, and T. P. Ward are gratefully acknowledged. We also thank J. T. Wasson for generously providing a sample of Filomena. This research was supported by funds from the Louis Block Fund of the University of Chicago and from the National Aeronautics and Space Administration through grants NAG 9-54 (to L. Grossman) and NAG 9-43 (to G. J. Wasserburg). This is Caltech Division of Geological and Planetary Sciences Contribution (4894) (708).

Editorial handling: R. A. Schmitt

REFERENCES

ANDERS E. and GREVESSE N. (1989) Abundances of the elements: Meteoritic and solar. *Geochim. Cosmochim. Acta* **53,** 197–214.

ARMSTRONG J. T. (1982) New ZAF and a-factor correction procedures for the quantitative analysis of individual microparticles. In *Microbeam Analysis/1982* (ed. K. F. J. HEINRICH), pp. 175–180. San Francisco Press.

ARMSTRONG J. T. (1984) Quantitative analysis of silicate and oxide minerals: A re-evaluation of ZAF corrections and proposal for new Bence-Albee coefficients. In *Microbeam Analysis/1984* (eds. A. ROMIG and J. I. GOLDSTEIN), pp. 208–212. San Francisco Press.

ARMSTRONG J. T., EL GORESY A., and WASSERBURG G. J. (1985) Willy: A prize noble Ur-Fremdling—Its history and implications for the formation of Fremdlinge and CAI. *Geochim. Cosmochim. Acta* **49,** 1001–1022.

ARMSTRONG J. T., HUTCHEON I. D., and WASSERBURG G. J. (1987) Zelda and company: Petrogenesis of sulfide-rich Fremdlinge and constraints on solar nebular processes. *Geochim. Cosmochim. Acta* **51,** 3155–3173.

ATKINS D. H. F. and SMALES A. A. (1960) The determination of tantalum and tungsten in rocks and meteorites by neutron activation analysis. *Anal. Chim. Acta* **22,** 462–478.

BARRETT C. and MASSALSKI T. B. (1980) *Structure of Metals.* Pergamon Press.

BECKETT J. R. and GROSSMAN L. (1986) Oxygen fugacities in the solar nebula during crystallization of fassaite in Allende inclusions (abstr.). *Lunar Planet. Sci. Conf. XVII,* 36–37.

BENCE A. E. and ALBEE A. L. (1968) Empirical correction factors for the electron microanalysis of silicates and oxides. *J. Geol.* **76,** 382–403.

BERLINCOURT L. E., HUMMEL H. H., and SKINNER B. J. (1981) Phases and phase relations of the platinum-group elements. In *Platinum-Group Elements: Mineralogy, Geology, Recovery* (ed. L. J. CABRI), pp. 19–45. Canadian Institute of Mining and Metallurgy.

BISCHOFF A. and PALME H. (1987) Composition and mineralogy of refractory-metal-rich assemblages from a Ca, Al-rich inclusion in the Allende meteorite. *Geochim. Cosmochim. Acta* **51,** 2733–2748.

BLANDER M., FUCHS L. H., HOROWITZ C., and LAND R. (1980) Primordial refractory metal particles in the Allende meteorite. *Geochim. Cosmochim. Acta* **44,** 217–223.

BLUM J. D., WASSERBURG G. J., HUTCHEON I. D., BECKETT J. R., and STOLPER E. M. (1989) Origin of opaque assemblages in C3V meteorites: Implications for nebular and planetary processes. *Geochim. Cosmochim. Acta* **53,** 545–558.

BOYNTON W. V. (1975) Fractionation in the solar nebula: condensation of yttrium and the rare earth elements. *Geochim. Cosmochim. Acta* **39,** 569–584.

CAILLET C., GOLDSTEIN J. I., VELDE D., and EL GORESY A. (1988) Estimation of possible thermal history of a Vigarano CAI (abstr.). *Meteoritics* **23,** 262–263.

CHASE M. W. JR., DAVIES C. A., DOWNEY J. R. JR., FRURIP D. J., MCDONALD R. A., and SYVERUD A. N. (1985) *JANAF Thermochemical Tables,* 3rd edn; *J. Phys. Chem. Ref. Data* **14,** Supp. 1.

CHOU C.-L., BAEDECKER P. A., and WASSON J. T. (1976) Allende inclusions: volatile-element distribution and evidence for incomplete volatilization of presolar solids. *Geochim. Cosmochim. Acta* **40,** 85–94.

DAVIS A. M. and GROSSMAN L. (1979) Condensation and fractionation of rare earths in the solar nebula. *Geochim. Cosmochim. Acta* **43,** 1611–1632.

DAVIS A. M., TANAKA T., GROSSMAN L., LEE T., and WASSERBURG G. J. (1982) Chemical composition of HAL, an isotopically-unusual Allende inclusion. *Geochim. Cosmochim. Acta* **46,** 1627–1651.

EKAMBARAM V., KAWABE I., TANAKA T., DAVIS A. M., and GROSSMAN L. (1984) Chemical compositions of refractory inclusions in

the Murchison C2 chondrite. *Geochim. Cosmochim. Acta* **48,** 2089–2105.

EL GORESY A., NAGEL K., and RAMDOHR P. (1978) Fremdlinge and their noble relatives. *Proc. 9th Lunar Planet. Sci. Conf.*, 1279–1303.

FEGLEY B. JR. and PALME H. (1985) Evidence for oxidizing conditions in the solar nebula from Mo and W depletions in refractory inclusions in carbonaceous chondrites. *Earth Planet. Sci. Lett.* **72,** 311–326.

FUCHS L. H. and BLANDER M. (1980) Refractory metal particles in refractory inclusions in the Allende meteorite. *Proc. 11th Lunar Planet. Sci. Conf.*, 929–944.

GROSSMAN L. (1972) Condensation in the primitive solar nebula. *Geochim. Cosmochim. Acta* **36,** 597–619.

GROSSMAN L. (1973) Refractory trace elements in Ca, Al-rich inclusions in the Allende meteorite. *Geochim. Cosmochim. Acta* **37,** 1119–1140.

GROSSMAN L. (1980) Refractory inclusions in the Allende meteorite. *Ann. Rev. Earth Planet. Sci.* **8,** 559–608.

GROSSMAN L. and GANAPATHY R. (1976) Trace elements in the Allende meteorite—I. Coarse-grained, Ca-rich inclusions. *Geochim. Cosmochim. Acta* **40,** 331–344.

GROSSMAN L. and OLSEN E. (1974) Origin of the high-temperature fraction of C2 chondrites. *Geochim. Cosmochim. Acta* **38,** 173–187.

GROSSMAN L., GANAPATHY R., and DAVIS A. M. (1977) Trace elements in the Allende meteorite—III. Coarse-grained inclusions revisited. *Geochim. Cosmochim. Acta* **41,** 1647–1664.

GROSSMAN L., DAVIS A. M., EKAMBARAM V., ARMSTRONG J. T., HUTCHEON I. D., and WASSERBURG G. J. (1986) Bulk chemical composition of a Fremdling from an Allende Type B inclusion (abstr.). *Lunar Planet. Sci. XVII,* 295–296.

HARA T. and SANDELL E. B. (1960) Meteoritic abundance of ruthenium. *Geochim. Cosmochim. Acta* **21,** 145–150.

HERR W., HOFFMEISTER W., HIRT B., GEISS J., and HOUTERMANS F. G. (1961) Versuch zur Datierung von Eisenmeteoriten nach der Rhenium-Osmium-Methode. *Z. Naturforsch.* **16a,** 1053–1058.

HULTGREN R., DESAI P. D., HAWKINS D. T., GLEISEN M., KELLY K. K., and WAGMAN D. D. (1973) *Selected Values of the Thermodynamic Properties of the Elements.* American Society for Metals.

HUTCHEON I. D., ARMSTRONG J. T., and WASSERBURG G. J. (1987) Isotopic studies of Mg, Fe, Mo, Ru and W in Fremdlinge from Allende refractory inclusions. *Geochim. Cosmochim. Acta* **51,** 3175–3192.

KÖHLER A. V., PALME H., SPETTEL B., and FEGLEY B. (1988) Fractionation of refractory metals by high temperature oxidation (abstr.). *Lunar Planet. Sci. XIX,* 627–628.

LATTIMER J. M. and GROSSMAN L. (1978) Chemical condensation sequences in supernova ejecta. *The Moon and Planets* **19,** 169–184.

LOVE G. and SCOTT V. D. (1978) Evaluation of a new correction procedure for quantitative electron probe microanalysis. *J. Phys.* **D 11,** 1369–1376.

MAO X.-Y., WARD B. J., GROSSMAN L., and MACPHERSON G. J. (1990) Chemical compositions of refractory inclusions from the Vigarano and Leoville carbonaceous chondrites. *Geochim. Cosmochim. Acta* **54,** 2121–2132.

MASSALSKI T. B. (1986) *Binary Alloy Phase Diagrams.* Amer. Soc. Metals.

MEEKER G. P., WASSERBURG G. J., and ARMSTRONG J. T. (1983) Replacement textures in CAI and implications regarding planetary metamorphism. *Geochim. Cosmochim. Acta* **47,** 707–721.

NICHIPORUK W. and BROWN H. (1965) The distribution of platinum and palladium metals in iron meteorites and in the metal phase of ordinary chondrites. *J. Geophys. Res.* **70,** 459–470.

PACKWOOD R. H. and BROWN J. D. (1981) A Gaussian expression to describe $\phi(\rho z)$ curves for electron probe microanalysis. *X-ray Spectrometry* **10,** 138–146.

PALME H. and WLOTZKA F. (1976) A metal particle from a Ca-Al-rich inclusion from the meteorite Allende, and condensation of refractory siderophile elements. *Earth Planet. Sci. Lett.* **33,** 45–60.

PALME H., LARIMER J. W., and LIPSCHUTZ M. E. (1988) Moderately volatile elements. In *Meteorites and the Early Solar System* (eds. J. F. KERRIDGE and M. S. MATTHEWS), pp. 436–461. Univ. of Arizona Press.

PALME H., HUTCHEON I. D., and SPETTEL B. (1989) The bulk composition of "Fremdlinge" from a Ca, Al-rich Allende inclusion (abstr.). *Lunar Planet. Sci. XX,* 814–815.

PAQUE J. M. (1989) Vanadium-rich refractory platinum metal nuggets from a fluffy Type A inclusion in Allende (abstr.). *Lunar Planet. Sci. XX,* 822–823.

PERLMAN I. and ASARO F. (1969) Pottery analysis by neutron activation. *Archaeometry* **11,** 21–52.

PERLMAN I. and ASARO F. (1971) Pottery analysis by neutron activation. In *Science and Archaeology* (ed. R. H. BRILL), pp. 182–195. MIT Press.

PERNICKA E. and WASSON J. T. (1987) Ru, Re, Os, Pt and Au in iron meteorites. *Geochim. Cosmochim. Acta* **51,** 1717–1726.

SMALES A. A., MAPPER D., and FOUCHÉ K. F. (1967) The distribution of trace elements in iron meteorites, as determined by neutron activation. *Geochim. Cosmochim. Acta* **31,** 673–720.

SYLVESTER P., WARD B. J., and GROSSMAN L. (1989) Chemical compositions of Fremdlinge from an Allende inclusion (abstr.). *Meteoritics* **24,** 330–331.

TYLKINA M. A. and SAVITSKII E. M. (1978) The present state of the rhenium problem and new directions in the development of alloys. In *Study and Use of Rhenium Alloys* (eds. E. M. SAVITSKII and M. A. TYLKINA), pp. 3–30. Amerind.

WARK D. A. (1986) Evidence for successive episodes of condensation at high temperature in a part of the solar nebula. *Earth Planet. Sci. Lett.* **77,** 129–148.

WASSON J. T. and WANG J. (1986) A nonmagmatic origin of group IIE iron meteorites. *Geochim. Cosmochim. Acta* **50,** 725–732.

WASSON J. T., OUYANG X., WANG J., and JERDE E. (1989) Chemical classification of iron meteorites: XI. Multi-element studies of 38 new irons and the high abundance of ungrouped irons from Antarctica. *Geochim. Cosmochim. Acta* **53,** 735–744.

WILLIS J. (1981) Antimony in iron meteorites. *Earth Planet. Sci. Lett.* **53,** 1–10.

ZINNER E. and EL GORESY A. (1990) Evidence for an extraneous origin of a periclase-metal Fremdling from the Vigarano CV3 chondrite. *Earth Planet. Sci. Lett.* (submitted).